[Papers in Palaeontology, 2024, e1562]

The virtual brain endocast of *Incamys bolivianus*: insight from the neurosensory system into the adaptive radiation of South American rodents

by ORNELLA C. BERTRAND[1,2,3,*], MADLEN M. LANG[4], JOSÉ D. FERREIRA[5], LEONARDO KERBER[5,6], ZOI KYNIGOPOULOU[2] *and* MARY T. SILCOX[4]

[1]Institut Català de Paleontologia Miquel Crusafont (ICP-CERCA), Universitat Autònoma de Barcelona, Edifici ICTA-ICP, c/ Columnes s/n, Campus de la UAB, Cerdanyola del Vallès (Barcelona) 08193, Spain; ornella.bertrand@icp.cat
[2]School of GeoSciences, University of Edinburgh, Grant Institute, Edinburgh, Scotland, UK
[3]Section of Mammals, Carnegie Museum of Natural History, Pittsburgh, Pennsylvania, USA
[4]Department of Anthropology, University of Toronto Scarborough, Toronto, Ontario, Canada
[5]Programa de Pós-Graduação em Biodiversidade Animal, Centro de Ciências Naturais e Exatas, Universidade Federal de Santa Maria, Santa Maria, Brazil
[6]Centro de Apoio à Pesquisa Paleontológica, Centro de Ciências Naturais e Exatas, Universidade Federal de Santa Maria, Santa Maria, Brazil
*Corresponding author

Typescript received 21 December 2023; accepted in revised form 23 April 2024

Abstract: Caviomorph rodents are endemic to South America and are one of the most adaptively diverse radiations of rodents today. Although their origin and diversification have been intensively studied, questions still remain about many of the details of where, when and how the group radiated. One area of continuing debate relates to the evolution of their neurosensory system. Modern caviomorphs exhibit a rich brain shape and size diversity. So far the oldest species for which endocranial data are known is dated to the Early Miocene. Here, we describe the virtual brain endocast of the late Oligocene stem chinchillid *Incamys bolivianus* from Bolivia and provide new hypotheses regarding the ancestral brain of Chinchillidae and Caviomorpha more broadly. Caviomorph rodents, independent from other rodent clades, acquired an expanded neocortex and their common ancestor was probably lissencephalic or had few sulci. *Incamys* uniquely combines extended neocortical temporal lobes and exposed caudal colliculi, which have roles in audition and vocalization processing. We interpret this morphology as evidence for enhanced auditory acuity, vocalization processing and potentially group-living in *Incamys*, which is known in modern members of the Chinchillidae family. No temporal effect was found on relative brain size in South American mammals; however, our sample is limited to available brain endocasts and as such remains small and unevenly distributed taxonomically and temporally. *Incamys* provides crucial insight into the evolution of the caviomorph brain and shows that we still have much to explore regarding how these small mammals achieved one the most impressive adaptive radiations of the Cenozoic.

Key words: endocast, brain, South America, caudal colliculi, Chinchillidae, Caviomorpha.

CAVIOMORPHA is one of the most successful groups of rodents today and is composed of four superfamilies, 11 families and more than 244 extant species (Huchon & Douzery 2001; Upham & Patterson 2015). Caviomorpha's closest relatives are Hystricidae and Phiomorpha from Africa and Asia (Upham & Patterson 2015). They are endemic to South America, but their ancestors immigrated from Africa, probably during the Eocene (Antoine *et al.* 2012; Vucetich *et al.* 2015a; Arnal *et al.* 2022), via one or more crossings of the South Atlantic (which would have been *c.* 1000–1500 km wide; Houle 1999). This group of rodents is also extremely ecologically diverse, displaying arboreal, terrestrial, fossorial, subterranean and aquatic adaptations (Verzi *et al.* 2010; Candela *et al.* 2012; Álvarez & Arnal 2015; Patton *et al.* 2015; Álvarez & Ercoli 2017; Kerber *et al.* 2022). One of the reasons for their incredible evolutionary success may come from the fact that they evolved in isolation on an island continent for *c.* 40 myr during the Cenozoic, enabling them to invade a plethora of ecological niches (Upham & Patterson 2015; Vucetich *et al.* 2015a; Boivin *et al.* 2018; Arnal *et al.* 2020, 2022). They are also distinct from other rodents in having a precocial mode of development, in which young are more developed at birth (Sibly & Brown 2009). A marked size disparity also exists among caviomorphs. Caviidae and

doi: 10.1002/spp2.1562

Chinchillidae encompass the largest rodents that ever lived, including the largest living rodent, the capybara (*Hydrochoerus*), averaging *c.* 60–70 kg and the extinct Pliocene Dinomyidae *Josephoartigasia monesi* (1200 kg with a standard deviation of 753 kg), which is the largest rodent known (Rinderknecht & Blanco 2008; Ferreira *et al.* 2020). At the other end of the size scale, there are several species with an average body mass of <100 g (Álvarez *et al.* 2017).

The palaeontological record of caviomorphs is rich and fossils have been recovered from Argentina, Bolivia, Brazil, Chile, Colombia, Peru, Uruguay, Venezuela, Central America and some Caribbean Islands, Mexico and the USA (e.g. Marshall *et al.* 1983; Pascual *et al.* 1996; Bertrand *et al.* 2012; Vucetich *et al.* 2015a, 2015b; Marivaux *et al.* 2020). There is a better understanding of the phylogenetic relationships among crown clades (i.e. Erethizontoidea, Cavioidea, Chinchilloidea and Pan-Octodontoidea) than within stem lineages, which do not belong to any modern groups (Antoine *et al.* 2012; Arnal & Vucetich 2015; Upham & Patterson 2015; Boivin *et al.* 2019).

One aspect that has been relatively understudied relates to the evolution of their neurosensory system and specifically their brain evolution. In the last couple of years, *c.* 60 virtual brain endocasts for extant caviomorph rodents have been published (Ferreira *et al.* 2020, 2022; Piñero *et al.* 2021; Lang *et al.* 2022; Arnaudo & Arnal 2023; Fernández Villoldo *et al.* 2023) as well as for three fossils, including the Late Miocene Chinchilloidea, *Neoepiblema acreensis*, and Cavioidea, *Neoreomys australis* (Ferreira *et al.* 2020), and the Early Miocene stem Pan-Octodontoidea, *Prospaniomys priscus* (Arnaudo & Arnal 2023). A few other natural endocasts have also been described: the Erethizontoidea, *Hypsosteiromys* sp., the Chinchilloidea, Cephalomyidae indet., the Pan-Octodontoidea, *Metacaremys primitiva,* all from the Miocene, *Prodolichotis prisca* and *Neocavia lozanoi* from the Late Miocene to Early Pliocene and the Cavioidea, *Dolicavia minuscula* from the Pliocene (Dozo 1997a, 1997b; Dozo *et al.* 2004; Madozzo-Jaén 2019; Piñero *et al.* 2021).

Although these various specimens have been informative about aspects of the diversification of the group, there is a gap corresponding to the first 20 myr of the brain evolution of the group. The main reason for this gap is the relative lack of complete crania for species older than the Early Miocene. Here we describe the brain virtual endocast of *Incamys bolivianus* (YPM VPPU 21945) from the late Oligocene of Bolivia. This specimen was described in 1982 by Patterson & Wood, who at the time considered it a fossil Cavioidea. Lavocat (1976) originally assigned the genus *Incamys* to Dasyproctidae (Cavioidea); however, cranial features such as the large size of the incisive foramen, located on the premaxilla–maxillary suture, suggest that this genus is not a dasyproctid. In *Dasyprocta* and *Myoprocta* the foramen is smaller and located behind the suture. Additionally, dental characteristics related to the pattern of reduction of the lophs and lophids and of enamel layer thinning more closely resemble the condition found in Chinchillidae (Chinchilloidea; Vucetich *et al.* 2015c). In the last decade, more material for Chinchilloidea has been found and refinement in phylogenetic analyses has led to a reconsideration of the phylogenetic position of *Incamys* (Vucetich *et al.* 2015c). *Incamys* is now considered a stem chinchillid, placed at the base of a group including extant Chinchillidae (Pan-Chinchillidae; Rasia & Candela 2019; Rasia *et al.* 2021).

Regardless of its phylogenetic position, *Incamys bolivianus* represents the oldest virtual endocast for a fossil caviomorph and provides crucial insight into the evolution of the neurosensory system of the group. Crown Chinchilloidea probably originated in the late Eocene to early Oligocene and *Incamys* is one of several Oligocene taxa recovered as stem chinchillids (Rasia *et al.* 2021). Remains of *I. bolivianus* have been found in Bolivia (Salla; Hoffstetter & Lavocat 1970) and in Argentina (Cabeza Blanca; Busker & Dozo 2017). There are no postcrania known for the genus and its diet has never been evaluated. Extant Chinchillidae are found in dry environments in the western and southern parts of South America. They are native to areas spanning the highlands of Ecuador to the Andes of Peru and Bolivia. They are also present in the coastal mountains of Chile and the steppe of Patagonia in Argentina (Patton *et al.* 2015). This group includes three genera: *Chinchilla*, *Lagidium* and *Lagostomus*. The first two can be considered rock-dwellers and jumpers while the last is a digger (Elissamburu & Vizcaíno 2004). In terms of diet, *Chinchilla* feeds on grass, stems and leaves, depending on the species, and the two other genera of the group eat grass (Álvarez *et al.* 2020). *Chinchillas* are relatively agile and use their long limbs to jump in rocky landscapes. *Lagidium peruanum* is also quite agile, but is more similar to rabbits in terms of its locomotor behaviour (Patton *et al.* 2015). *Chinchilla lanigera* produces many vocalizations (Spotorno *et al.* 2004). *Lagidium peruanum* uses calls (= whistles) to communicate with other members of the groups, and different whistles may correspond to different predators (Patton *et al.* 2015). *Lagostomus* lives in an expanded network of burrows and tunnels. They have an extensive range of vocalizations including calls given in response to a predator presence, when female members forage or during male–male interactions (Jackson *et al.* 1996; Patton *et al.* 2015).

Mammals other than rodents were also living in complete isolation in South America during part of the

Cenozoic, at least until the Miocene (Chávez Hoffmeister 2020), and this isolation is likely to have had a crucial impact on their evolution as well, with the emergence of endemic groups such as the Meridiungulata including notoungulates (Giannini & García-López 2014). Brain virtual endocasts have been generated for other South American mammals besides rodents including primates, xenarthrans, notoungulates and litopterns (e.g. Tambusso & Fariña 2015a; Ni *et al.* 2019; Dozo *et al.* 2023; Martínez *et al.* 2023). The physical environment has also been shown to play a crucial role in the brain evolution of mammals, such as the impact of invading a new niche (Sol *et al.* 2008), the climate cooling starting during the Oligocene in North America (Bertrand *et al.* 2021), and the end-Cretaceous extinction (Bertrand *et al.* 2022).

The goal of this study is to add fundamental and needed knowledge on the neurosensory system of fossil caviomorphs so that we can more accurately interpret the evolution of the diversity present in modern members of this group. Previous studies have started to tackle the question of the neurosensory diversity present in modern Caviomorpha (Ferreira *et al.* 2020, 2022; Arnaudo & Arnal 2023; Fernández Villoldo *et al.* 2023), but much remains to be clarified. *Incamys* preserves the oldest brain endocast for a caviomorph rodent; therefore, its anatomical description is crucial to provide new insight into the brain evolution of the group. Beyond anatomical descriptions, another goal is to quantify the relative size changes in the brain and its components to identify any neurosensory trends through time in Caviomorpha. Finally, we incorporate published quantitative data of other South American mammals to investigate the range of size variation of the brain and components from the Oligocene to the Pleistocene in order to better understand the impact of endemism on the brain evolution of South American mammals.

Institutional abbreviations. AMNH, American Museum of Natural History, New York, NY, USA; AMNH F:AM, Frick collection, American Museum of Natural History, New York, NY, USA; MACN-PV CH, Vertebrate Paleontology Collection, Museo Argentino de Ciencias Naturales 'Bernardino Rivadavia', Buenos Aires, Argentina; MCN-D, Mammal collection of the Fundação Zoobotânica do Rio Grande do Sul, Brazil; MMP, Museo Municipal de Ciencias Naturales de Mar del Plata, Argentina; NMB, Naturhistorisches Museum Basel, Switzerland; PIMUZ A/V, Paleontological Institute and Museum, University of Zurich, Switzerland; ROMV, Royal Ontario Museum Vertebrate Paleontology, Toronto, Canada; UFAC, Paleontological collection of the Universidade Federal do Acre (Campus Rio Branco), Brazil; UM, University of Michigan, Ann Arbor, MI, USA; USNM, United States National Museum of Natural History, Washington DC, USA; YPM VP, Yale Peabody Museum Vertebrate Paleontology, New Haven, CT, USA; YPM VPPU, Yale Peabody Museum Vertebrate Paleontology (Princeton University collection), New Haven, CT, USA.

MATERIAL AND METHOD

Incamys bolivianus (YPM VPPU 21945) was discovered in the Salla-Luribay Basin in Bolivia (Hoffstetter & Lavocat 1970). This site is dated to the late Oligocene and more specifically to the Deseadan (SALMA; South American Land Mammal Age; Kay *et al.* 1998; Dunn *et al.* 2013; Pérez *et al.* 2019), providing an age of 27.5–26.2 Ma (Vandenberghe *et al.* 2012). The skull is relatively complete and only a small portion of the rostrum is missing (Fig. 1A). This skull was illustrated and described in detail by Patterson & Wood in 1982. The cranium and mandible are attached to one another by sediment and the upper and lower teeth are in occlusion.

Comparative sample

We made anatomical comparisons of the brain endocast of *I. bolivianus* with relatively closely related taxa. The genus *Incamys* has been identified as a stem Chinchillidae in a recent phylogenetic analysis (Rasia *et al.* 2021), therefore, we compared it with the modern Chinchillidae: *Chinchilla lanigera* (Fig. 1B; AMNH 180038), *Lagidium peruanum* (Fig. 1C; NMB 1043) and *Lagostomus maximus* (Fig. 1D; AMNH 41523). Quantitative data have been published for both virtual endocasts of *Chinchilla* and *Lagostomus* by Lang *et al.* (2022). Dinomyidae is the sister-clade to Chinchillidae, therefore we also made comparisons to the only living chinchilloid outside of Pan-Chinchillidae: *Dinomys branickii* (MCN-D 072), and the Late Miocene fossil, *Neoe. acreensis* (UFAC 4515) from Brazil, for which endocranial data have been published (Ferreira *et al.* 2020). We elected to make additional anatomical comparisons with two other fossil caviomorph rodents from the Early Miocene: the Cavioidea, *Neor. australis* (PIMUZ A/V 5265; Ferreira *et al.* 2020), and the Octodontoidea, *Prospaniomys priscus* (MACN-PV CH1913; Arnaudo & Arnal 2023), both from Argentina and for which virtual brain endocasts have been produced. When possible, we made some anatomical comparisons with published natural endocasts: the Erethizontoidea, *Hypsosteiromys* sp., the Chinchilloidea, Cephalomyidae indet., the Cavioidea, the Pan-Octodontoidea, *Me. primitiva* from the Miocene, *Do. minuscula* from the Pliocene and *Prod. prisca* from the Late Miocene to Early Pliocene (Dozo 1997a, 1997b; Dozo *et al.* 2004; Madozzo-Jaén 2019; Piñero *et al.* 2021).

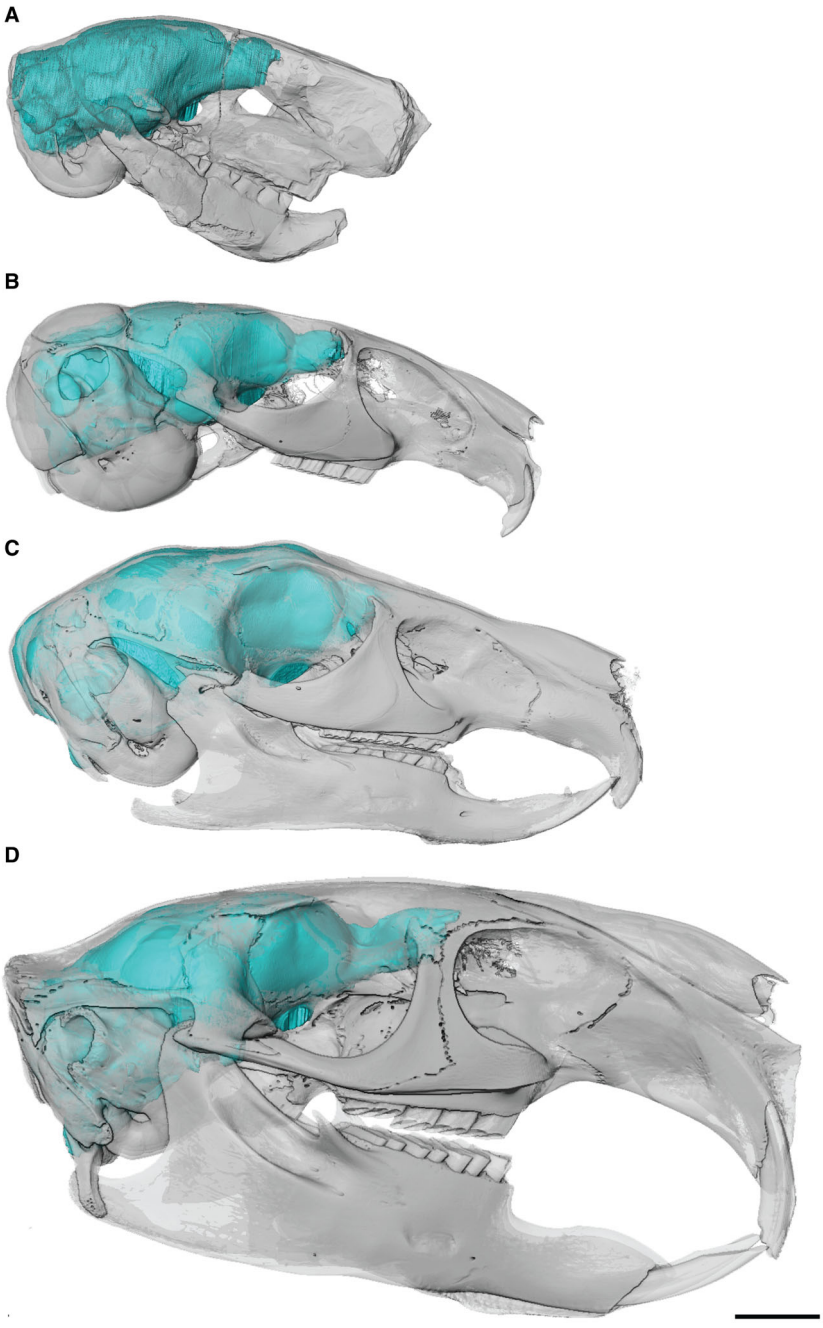

FIG. 1. Virtual endocasts inside the cranium of fossil and extant Chinchillidae. A, *Incamys bolivianus* (YPM VPPU 21945). B, *Chinchilla lanigera* (AMNH 180038). C, *Lagidium peruanum* (NMB 1043). D, *Lagostomus maximus* (AMNH 41523). Scale bar represents 10 mm.

Regarding quantitative comparisons, we made comparisons with contemporary North American and European Oligocene Ischyromyidae (*Ischyromys typus*) and Sciuroidea from the Oligocene (*Cedromus wilsoni*, *Prosciurus relictus*, *Protosciurus* cf. rachelae) and the Miocene (*Miopetaurista crusafonti*, *Mesogaulus paniensis*), for which brain endocasts have been described (Bertrand & Silcox 2016; Bertrand *et al.* 2017, 2018), and other South American mammals (Table S1) spanning the Oligocene to the Pleistocene including the Caviomorpha, *Do. minuscula* (Dozo 1997a), Notoungulata (Dozo & Martínez 2016; Fernández-Monescillo *et al.* 2019; Martínez *et al.* 2019; Perini *et al.* 2022; Martínez *et al.* 2023), Litopterna (Dozo *et al.* 2023), Primates, *Chilecebus carrascoensis* (Ni *et al.* 2019), and Xenarthra (Tambusso & Fariña 2015a, 2015b). All fossils included in the quantitative analyses are known from published virtual endocasts except *Do. minuscula*, which is a natural endocast.

Virtual endocast acquisition

The skull of *I. bolivianus* was scanned in 2014 at the Shared Materials Instrumentation Facility (SMIF), Duke University (North Carolina, USA) with a high-resolution x-ray micro-computed tomography (CT) scanner with a source–object distance of 120.96 mm and energy settings of 194 kV and 68 μA. The voxels are isotropic and voxel size is 0.028088 mm. The cranium of *Lagi. peruanum* (Fig. 1C) was scanned using a Nikon XT H 225 ST at the facilities of the Anthropological Department of the University of Zurich in Switzerland, with a source–object distance of 237.18 mm and a voxel size of 0.040494 mm. A virtual brain endocast for this specimen was generated for this study and is available in MorphoSource (Table S2). The virtual endocasts of *C. lanigera* (Fig. 1B) and *Lago. maximus* (Fig. 1D) have already been published (Lang *et al.* 2022) (Table S2).

The specimen of *I. bolivianus* was originally segmented in ImageJ using a WACOM Cintiq 21UX tablet. For each slice, the inside of the endocranial cavity was filled in pure white, which enabled visualization of the endocast separately from the cranium. In instances in which the bone was not preserved, a straight line was drawn to link the two nearest pieces of bone. Then, the filled stack was opened in Avizo v9.7.0 software (Visualization Sciences Group 1995–2019) for visualization. A new labelfield module was generated in the 'segmentation' tab where some areas of the endocranial reconstruction were refined (e.g. canals for vessels). Then, a surface rendering of the endocast was produced using unconstrained smoothing. To estimate the volume of the endocast, the module 'generate surface' was used. The specimen of *Lagi. peruanum* (Fig. 1C) was segmented using a semi-automatic method. First, we filled the endocranial cavity in 20 slices that were located equidistant from one another along the entire endocranial cavity to generate a labelfield module. Then, we used the Biomedisa application (Lösel *et al.* 2020) to segment the rest of the endocranial space. We uploaded the slices saved as a single .tif file, along with the labelfield module generated in Avizo. Biomedisa detects the difference in density between the bone and the cavity, therefore rendering the process of segmentation more efficient than interpolating in Avizo. Once the segmentation was complete in Biomedisa, we uploaded the result to Avizo to refine the segmentation, especially with respect to the different openings (i.e. foramina and cribriform plate) into the endocranial cavity to generate a more polished version. The virtual brain endocast of *C. lanigera* and *Lago. maximus* (Fig. 1B, D) was segmented in Avizo. A new labelfield module was created and the endocranial cavity was selected using the magic wand tool. The different openings of the cranium were closed manually using straight lines.

Palaeobiological calculations

Body mass estimation. Because no postcranial material has been recovered for *I. bolivianus*, we used an equation based on cranial dimensions to estimate its body mass (Tables 1, S1). Cranial length is considered the most reliable proxy (Bertrand *et al.* 2016a), but because the rostrum was incomplete, we used cheek-tooth area instead (Body mass = $10^{(((\log_{10}(\text{cheek-tooth area})) \times 1.6137) + 0.1606)}$, which is the second most correlated cranial dimension to body mass in rodents (Bertrand *et al.* 2016a). We used the same equation for all other compared fossil rodents for consistency except for *Protosciurus* cf. *rachelae* (YPM 14736), for which we used cranial length (Body mass = $10^{(((\log_{10}(\text{cranial length})) \times 3.9519) - 4.2316)}$ because of the incompleteness of the specimen (i.e. teeth not preserved).

Neurobiology. Linear measurements were recorded on the virtual endocast of *I. bolivianus*, *C. lanigera*, *Lago. maximus* and *Lagi. peruanum* following Bertrand & Silcox (2016). We produced ratios for some of the measurements (Table 1). The olfactory bulb volume for those specimens was estimated using the module 'volume edit' tool in Avizo by editing out the part of the endocast that was not olfactory bulbs. We generated the neocortical surface area for the same taxa as well as for the published *Neor. australis* and *Di. branickii*. We calculated the full neocortical surface area that included the superior sagittal sinus (Bertrand *et al.* 2018). We virtually extracted the neocortical surface area using the pen tool in Avizo. Finally, we estimated the volume of both petrosal lobules (= paraflocculi) in *I. bolivianus*, *C. lanigera*, *Lago. maximus*, *Lagi. peruanum* and *Neor. australis*. We used the segmentation tool to isolate the petrosal lobules from the rest of the endocast (Lang *et al.* 2022) and then we generated the volume in a similar manner to the way the volume of the entire endocast was generated. We also estimated the neocortical surface area and volume of the olfactory bulbs for the caviomorphs published in Lang *et al.* (2022). Volumetric and surface area measurements for the new specimens and the entire sample are listed in Tables 1 and S1.

Statistical analysis. We performed a series of statistical analyses for Caviomorpha and South American fossil mammals based on data gathered from the literature (Table S1). We investigated the relationship between the: (1) endocranial volume and body mass; (2) olfactory bulb volume and endocranial volume; (3) olfactory bulb volume and body mass; (4) petrosal lobule volume and endocranial volume; (5) petrosal lobule volume and body mass; and (6) neocortical surface area and endocranial surface area. Percentages of the size of the olfactory bulbs, petrosal lobules and neocortex, all relative to the endocranial volume or surface,

TABLE 1. Body mass estimates, linear measurements, volumes, surface areas, and encephalization quotients for the stem Chinchillidae *Incamys bolivianus* (YPM VPPU 21945) and extant Chinchillidae.

Measurements	*Incamys bolivianus* (YPM VPPU 21945)	*Lagostomus maximus* (AMNH 41523)	*Chinchilla lanigera* (AMNH 180038)	*Lagidium peruanum* (NMB 1043)
Cheek-teeth area (mm^2)	49.56	–	–	–
Body mass (g)	787.11	4859.68	442.70	1240.00
Linear measurements (mm)				
Total endocranial length (TL)	29.48	55.23	37.42	47.5
Olfactory bulb length (OL)	4.52	11.18	5.56	7.88
Olfactory bulb width (OW)	8.48	8.66	7.26	10.95
Olfactory bulb height (OH)	5.98	7.13	4.82	6.84
Cerebrum maximum length (CRML)	17.66	32.38	19.49	33.49
Cerebrum maximum width (CRMW)	22.74	33.98	24.75	31.93
Cerebrum maximum height (CRMH)	12.86	19.25	15.19	20.33
Cerebellum maximum length (CLML)	5.35	9.89	8.52	10.88
Cerebellum width (without paraflocculi) (CLW)	15.58	19.92	13.86	19.42
Cerebellum maximum width (CLWP)	19.9	24.19	19.69	25.48
Ratios of linear measurements (%)				
OL/TL	15.33	20.24	14.86	16.59
CRML/TL	59.91	58.63	52.08	70.51
CLML/TL	18.15	17.91	22.77	22.91
CLW/CRMW	68.51	58.62	56.00	60.82
OW/CRMW	37.29	25.49	29.33	34.29
OW/CLW	54.43	43.47	52.38	56.39
Surface areas (mm^2) and volumes (mm^3)				
Total endocranial surface area (TS)	2202.33	3899.19	2158.88	3631.73
Neocortical surface area (NS)	650.12	1565.02	638	1482.95
Total endocranial volume (TV)	3936.97	13 326.6	5602.95	12 618.3
Olfactory bulb volume (OV)	173.524	352.436	122.198	289.12
Left petrosal lobule volume	33.51	9.1	51.3	131.3
Right petrosal lobule volume	30.81	8.5	51.97	131.6
Total petrosal lobule volume (PV)	64.32	17.6	103.27	262.9
Ratios of surface areas and volumes (%)				
NS/TS	29.52	40.14	29.55	40.83
OV/TV	4.41	2.64	2.18	2.29
PV/TV	1.63	0.13	1.84	2.08
Encephalization quotient (Pilleri *et al.* 1984)	0.55	0.57	1.13	1.31

Body mass estimates for extant taxa are from Álvarez *et al.* (2017).

were generated. We elected to perform ordinary least squares (OLS) and phylogenetic generalized least squares (PGLS) linear regressions for: (1) extant Caviomorpha only; and (2) extant + fossil rodents to show the effect of phylogeny on the different allometric relationships (see Fig. S1 for the topology used in the PGLS regression). The resulting four regressions for each of the six relationships are presented in Table S3. For South American fossil mammals we used OLS linear regressions because the relationships among Notoungulata and Litopterna remain unclear (Martínez *et al.* 2023). All of the South American fossil taxa used in these analyses range from the Oligocene to the Pleistocene. For this sample, we investigated the following relationships: (1) endocranial volume and body mass; (2) olfactory bulb volume and endocranial volume; (3) olfactory bulb volume and body mass; and (4) neocortical surface area and endocranial surface area. These analyses resulted in four regressions in total (Table S4). All analyses were performed in R v3.6.2 (R Core Team 2019) and R studio v2023.06.2 (R Studio Team 2022).

We generated the residuals for the different relationships for the PGLS regression for the Rodentia-only set of analyses and the OLS regression for South American fossil mammals, using the function 'residuals' in the package stats v4.3.1 (Chambers & Hastie 1992). We then produced boxplots based on these residuals to compare *I. bolivianus* with extant caviomorphs, fossil ischyromyids and sciuroids as well as other South American fossil mammals. We also generated EQ values for *I. bolivianus* based on the Pilleri *et al.* (1984) equation that was

specifically designed for rodents (Table 1). Instead of plotting the EQ values, we choose to illustrate the residuals from the brain–body mass relationship in boxplots that shows similar results.

For all regressions, we used the function ggplot in the package ggplot2 v3.4.3 (Wickham 2016) for visualization and the function gls in the package nlme v3.1-162 (Pinheiro *et al.* 2023). Normality of the data was assessed using a Shapiro–Wilk test (data normally distributed: $p > 0.05$). The homogeneity of the variances (equality of the variance: $p > 0.05$) was verified using a Levene's test (when data were not normally distributed) or Bartlett's test (when data were normally distributed). In all but one case, variances were equal and we used Fisher–Pitman permutation tests with the functions oneway-test in the package coin v1.4-2 (Hothorn *et al.* 2006) and pairwisePermutationTest in the package rcompanion v2.4.30 (Mangiafico 2023). In the case of the neocortical surface area plotted against endocranial surface area for South American mammals, variances were not equal, therefore we used a Welch test (Welch 1951) and the functions welch.test and paircomp in the package onewaytests v2.7 (Dag *et al.* 2018). These tests enabled us to assess whether groups had significant differences in endocranial residuals but were performed only with more than two individuals per category (Tables S5, S6). Boxplots were created in the software R using the function ggboxplot in the package ggplot2 (Wickham 2016).

The lack of quantitative data on fossil caviomorphs prevents us from performing more sophisticated analyses such as ancestral state reconstruction, which could lead to misleading results. Additionally, because of the demonstrated temporal effect on relative brain size showing that Paleocene mammals had relatively smaller brains than Eocene taxa (Bertrand *et al.* 2022), we refrained from comparing more distantly related extant caviomorph rodents with a fossil chinchillid from the Oligocene. There could have been many instances of decrease and increase throughout the evolutionary history of each caviomorph suborders, which we cannot take into account because of the lack of fossil taxa for these groups. Endocranial data on South American mammals are rare and only endocranial volume is usually published. Therefore, we created distinct sample sizes for our different analyses given that data on parameters such as the size of the petrosal lobules have not been made available yet for any of the South American taxa except rodents.

DESCRIPTIONS AND COMPARISONS

Olfactory bulbs. The olfactory bulbs are almost completely preserved in *I. bolivianus* and only the ventral borders of the tips are difficult to distinguish because the bone is broken. In dorsal view (Fig. 2) the olfactory bulbs are narrower anteriorly compared with the posterior region, creating a triangular shape, and there is no gap separating the olfactory bulbs (Fig. 2A). In *C. lanigera* the bulbs are more elongate and less bulbous than in *Incamys* (Fig. 2B). The bulbs of *Lagi. peruanum* are relatively slightly shorter anteroposteriorly and less bulbous than in *I. bolivianus*, (Fig. 2C). There is no gap between the bulbs in either *Lagi. peruanum* or *C. lanigera*, similarly to *I. bolivianus* (Fig. 2B, C). *Neoreomys australis* (Ferreira *et al.* 2020, fig. S5) and *Pros. priscus* (Arnaudo & Arnal 2023, fig. 4.1) have a similar morphology to *C. lanigera*. The olfactory bulbs of *Lago. maximus* are relatively narrower and more elongate than in *I. bolivianus* (Fig. 2C). In contrast to *I. bolivianus*, there is a gap anteriorly between the bulbs in *Lago. maximus* (Fig. 2D). In *Di. branickii* the olfactory bulbs have similar dimensions anteroposteriorly as to *I. bolivianus*. Additionally, a gap is medially present on more than half of the anteroposterior length of the bulbs in this specimen (Ferreira *et al.* 2020, fig. S7). The olfactory bulbs of *Neoe. acreensis* and of the natural endocasts are not sufficiently preserved to enable a fair comparison of their shape.

The olfactory bulbs are positioned above the M2 in *I. bolivianus* (Fig. 1A), which is similar to the condition observed in *Di. branickii* (Ferreira *et al.* 2020, fig. 1). This contrasts with *C. lanigera* (AMNH 180038; Fig. 1B), *Lagi. peruanum* (Fig. 1C) and *Lago. maximus* (Fig. 1D), for which the olfactory bulbs are above the M1. The rostral aspect of the olfactory bulbs in *Pros. priscus* (Arnaudo & Arnal 2023, fig. 9.2) is at the posterior margin of the M1. For *Neoe. acreensis* the olfactory bulbs are not well preserved, but the rostral limit of the bulbs does not appear to go beyond M3 anteriorly (Ferreira *et al.* 2020, fig. S2). The condition cannot be determined in any of the natural endocasts.

The circular fissure is relatively narrow in *I. bolivianus*, *C. lanigera* and *Lagi. peruanum* (Figs 2, 3) compared with *Lago. maximus* in which the fissure is relatively more expanded anteroposteriorly (Figs 2, 3). The circular fissure is also narrow in *Di. branickii*, *Neoe. acreensis*, *Neor. australis* (Ferreira *et al.* 2020, fig. S2, S7, S8), and *Pros. priscus* (Arnaudo & Arnal 2023, fig. 4.3). Because of the state of preservation, the characteristics of this feature cannot be determined in the natural endocasts.

Cerebrum & midbrain. For this section, because of the limited preservation of the natural endocasts, they are mentioned only when a feature is visible on their surface. In dorsal view the anterior boundaries of cerebral hemispheres are rounded and separated medially by the superior sagittal sinus in between the hemispheres in *I. bolivianus* (Fig. 2A), *C. lanigera* (Fig. 2B), *Lagi. peruanum* (Fig. 2C), *Pros. priscus* (Arnaudo &

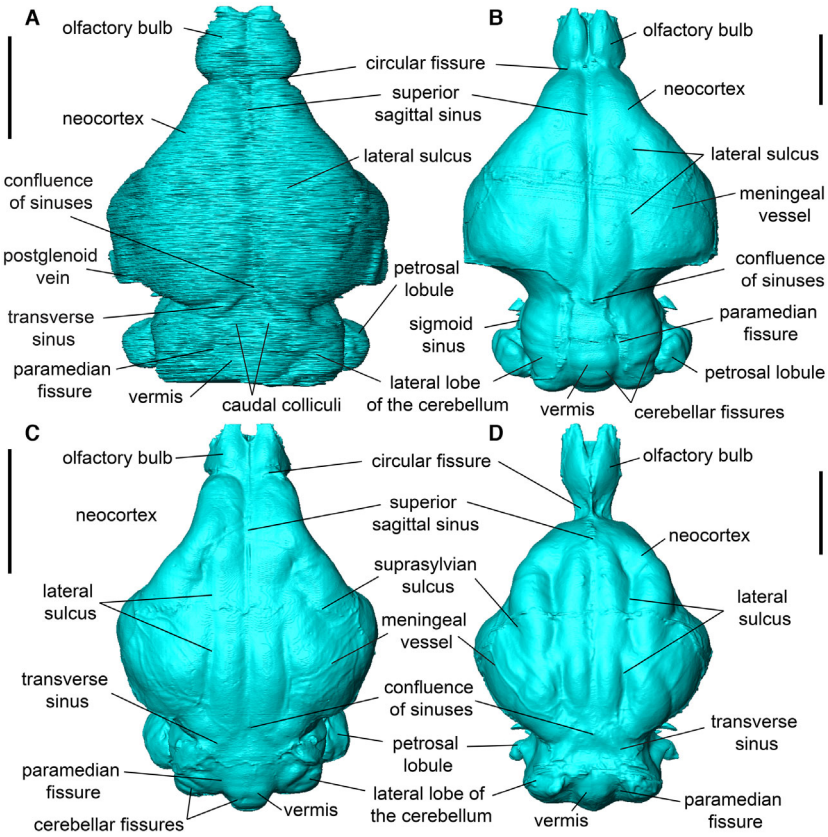

FIG. 2. Virtual reconstruction in dorsal view of the brain virtual endocasts of fossil and extant Chinchillidae. A, *Incamys bolivianus* (YPM VPPU 21945). B, *Chinchilla lanigera* (AMNH 180038). C, *Lagidium peruanum* (NMB 1043). D, *Lagostomus maximus* (AMNH 41523). Scale bars represent 10 mm.

Arnal 2023, fig. 4.1) and *Neor. australis* (Ferreira *et al.* 2020, fig. S8). This contrasts with *Lago. maximus*, in which the cerebral hemispheres are relatively straight anteriorly with no indentation for the superior sagittal sinus (Fig. 2D). In *Di. branickii* (Ferreira *et al.* 2020, fig. S7) the cerebral hemispheres are also rounded, but mediolaterally broader than the above taxa and the superior sagittal sinus is raised for the entire anteroposterior length of the cerebrum, while this is the case only anteriorly in *Pros. priscus*. For the latter, the posterior part of the superior sagittal sinus is buried between both hemispheres (Arnaudo & Arnal 2023, fig. 4.1). *Neoepiblema acreensis* shows the same condition as in *Di. branickii*; however, the anterior region of the cerebrum of *Neoe. acreensis* is not well-preserved (Ferreira *et al.* 2020, fig. S2, S7). In dorsal view the lateral borders of the anterior region of the cerebrum are slightly concave in *I. bolivianus* and *C. lanigera* (Fig. 2A, B), and even more so in *Lagi. peruanum* (Fig. 2C). The borders are more straight in *Pros. priscus* (Arnaudo & Arnal 2023, fig. 4.1), and more convex in *Lago. maximus* (Fig. 2D) and *Di. branickii* (Ferreira *et al.* 2020, fig. S7). No comparison can be made for *Neoe. acreensis* and *Neor. australis* because of deformation of this region. The temporal lobes extend further laterally relative to the anterior aspect of the cerebrum in *I. bolivianus*, all Chinchillidae taxa (Fig. 2), Cephalomyidae indet. (Dozo 1997b, fig. 1), *Dolicavia minuscula* (Dozo 1997a, fig. 1) and *Neor. australis* (Ferreira *et al.* 2020, fig. S8). This contrasts with *Di. branickii* (Ferreira *et al.* 2020, fig. S7), *Pros. priscus* (Arnaudo & Arnal 2023, fig. 4.1) and *Me. primitiva* (Piñero *et al.* 2021, fig. 2), in which this extension is less marked. The situation is unclear in *Neoe. acreensis* because the region is deformed (Ferreira *et al.* 2020, fig. S2). The anterior region of the cerebral hemispheres is broader than the posterior region in *Hypsosteiromys*, which contrasts with all other taxa. As in *I. bolivianus*, the superior sagittal sinus of *Hypsosteiromys* separated both hemispheres anteroposteriorly (Dozo *et al.* 2004, fig. 2). The cerebrum is not sufficiently preserved to enable comparisons with *Prod. prisca* (Madozzo-Jaén 2019, fig. 5).

On the ventral view of the cerebrum, the hypophyseal fossa for the pituitary gland has a convex and circular shape and is positioned posteriorly to the exit for V_3 in *I. bolivianus* (Fig. 4A). In *C. lanigera* this structure is

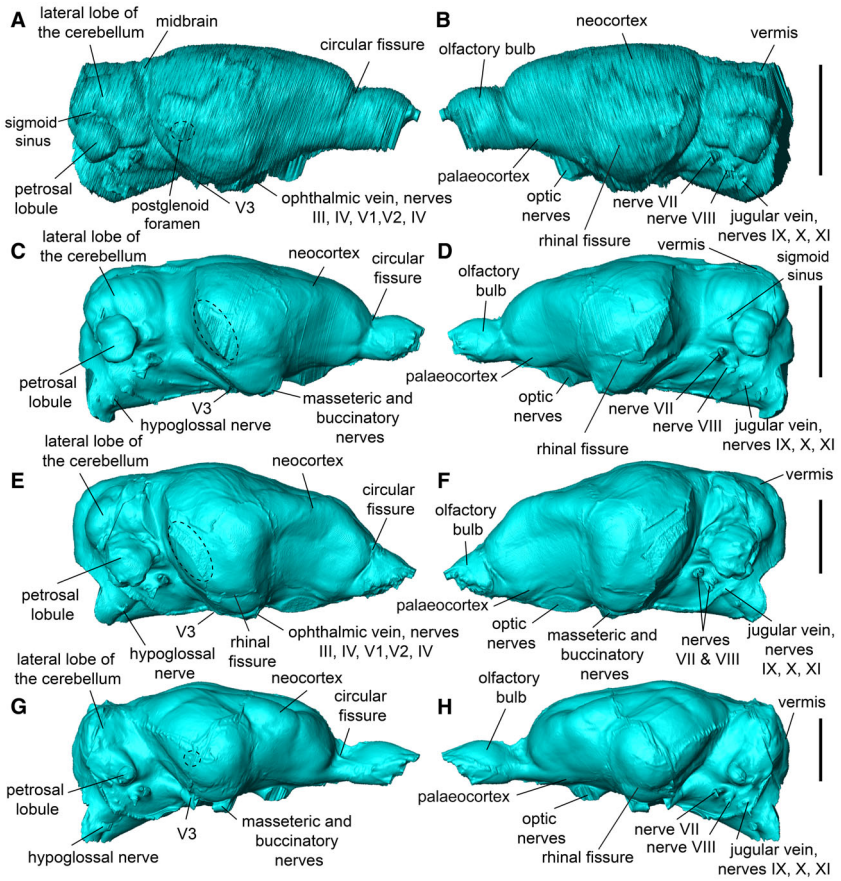

FIG. 3. Virtual reconstruction in lateral view of the brain virtual endocasts of fossil and extant Chinchillidae. A–B, *Incamys bolivianus* (YPM VPPU 21945). C–D, *Chinchilla lanigera* (AMNH 180038). E–F, *Lagidium peruanum* (NMB 1043). G–H, *Lagostomus maximus* (AMNH 41523). Dashed lines (A, C, E, F) represent the postglenoid foramen. Scale bars represent 10 mm.

more elongate anteroposteriorly and is positioned more anteriorly than in *I. bolivianus*, being anterior to the exit for nerve V_3 (Fig. 4B). The hypophyseal fossa of *Neor. australis* also appears to have been convex, but the deformation of the specimen prevents a more detailed description of its position and precise shape (Ferreira *et al.* 2020, fig. S8). This structure is not distinguishable or clearly delimited in *Lagi. peruanum* (Fig. 2C), *Lago. maximus* (Fig. 2D), *Di. branickii* (Ferreira *et al.* 2020, fig. S7) and *Pros. priscus* (Arnaudo & Arnal 2023, fig. 4.1). The preservation of this area is incomplete in *Neoe. acreensis*, (Ferreira *et al.* 2020, fig. S2).

The rhinal fissure corresponds to the anatomical landmark that separates the neocortex from the palaeocortex (= piriform lobe) in mammals (Martin 1990, pp. 357–426). The position of the rhinal fissure can provide information about the relative size of the neocortex (Jerison 2012; Long *et al.* 2015). In lateral view, the rhinal fissure is visible in *I. bolivianus* (Fig. 3) and extends anteroposteriorly along the cerebrum, just dorsal to the level of the ventral region of the olfactory bulbs. The posterior part of the rhinal fissure meets with the transverse sinus posteriorly. This configuration is similar in all compared virtual endocasts, but cannot be determined in the natural endocasts. In terms of the neocortical sulci, *I. bolivianus* has a lateral sulcus on each hemisphere (Figs 2A, S2) as in *C. lanigera* (Fig. 2B), *Lagi. peruanum* (Fig. 2C), *Lago. maximus* (Fig. 2D; Ferreira *et al.* 2020, fig. S6), *Di. branickii*, *Neoe. acreensis* (Ferreira *et al.* 2020, figs S2, S7), *Pros. priscus* (Arnaudo & Arnal 2023, fig. 4.1), *Prod. prisca* (Madozzo-Jaén 2019, fig. 5) and *Do. minuscula* (Dozo 1997a, fig. 1). The lateral sulcus appears to be absent in *Neor. australis* based on the state of preservation (Ferreira *et al.* 2020, fig. S8). A suprasylvian sulcus is present on both hemispheres in *Lagi. peruanum* (Fig. 2C), *Lago. maximus* (Fig. 2D; Ferreira *et al.* 2020, fig. S6), *Pros. priscus* (Arnaudo & Arnal 2023, fig. 4.3), *Neoe. acreensis*, *Di. branickii* (Ferreira *et al.* 2020, figs S2, S7) and *Do. minuscula* (Dozo 1997a, fig. 1), but absent in other taxa (i.e. *I. bolivianus*, *C. lanigera* and *Neor. australis*). *Hypsosteiromys* (Dozo *et al.* 2004, fig. 2) and Cephalomyidae indet. (Dozo 1997b, fig. 1) do not have any neocortical sulci.

In dorsal view the midbrain is not covered by the cerebrum in *I. bolivianus*, and a region of the midbrain, the caudal colliculi (= inferior colliculi; associated with acoustic reflexes; Christensen & Evans 1979)

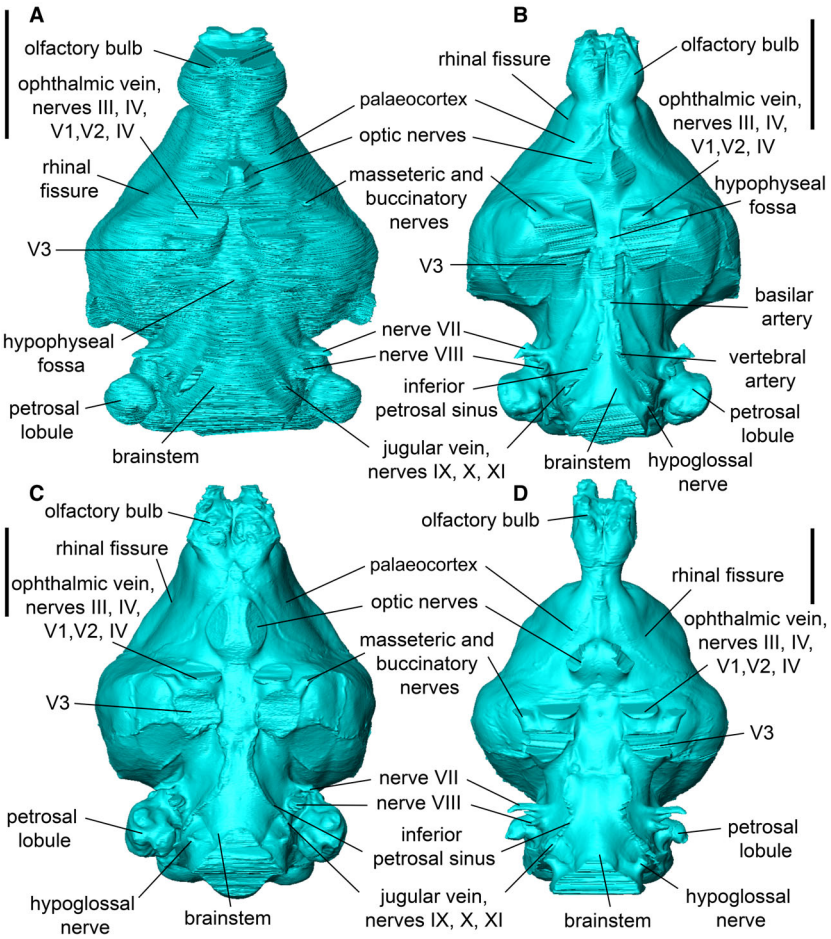

FIG. 4. Virtual reconstruction in ventral view of the brain virtual endocasts of fossil and extant Chinchillidae. A, *Incamys bolivianus* (YPM VPPU 21945). B, *Chinchilla lanigera* (AMNH 180038). C, *Lagidium peruanum* (NMB 1043). D, *Lagostomus maximus* (AMNH 41523). Scale bars represent 10 mm.

is visible (Figs 2A, S2). These structures are also visible in some other published fossil rodents: *Reithroparamys*, one specimen of *I. typus* (Bertrand & Silcox 2016; Bertrand *et al.* 2019), *Adelomys vaillanti* (Dechaseaux 1958), and *Pseudocylindrodon texanus* (Wood 1974). The midbrain is also visible in *Pros. priscus* (Arnaudo & Arnal 2023, fig. 4.1), but the caudal colliculi are not evident. However, this could be due to preservation (Arnaudo & Arnal 2023). The midbrain is covered by the cerebrum in *Do. minuscula* (Dozo 1997a, fig. 1) and all other well-preserved compared virtual endocasts. The condition of *Neor. australis* is uncertain because of poor preservation of the area (Ferreira *et al.* 2020, fig. S8). The condition of the midbrain cannot be determined for any of the other natural endocasts.

Cerebellum. The cerebellum, with the inclusion of the petrosal lobules, is mediolaterally narrower than the cerebrum in *I. bolivianus* (Fig. 2A; Table 1), a relationship that is similar to that in other compared virtual endocasts (Ferreira *et al.* 2020) and *Do. minuscula* (Dozo 1997a, fig. 1) except *Pros. priscus*, which has a cerebellum as wide as the cerebrum (Arnaudo & Arnal 2023, fig. 4.1). The paramedian fissures, which separate the lateral lobes of the cerebellum from the vermis laterally, are visible in dorsal and lateral views, in *I. bolivianus*, *Lagi. peruanum*, *C. lanigera* (Figs 2, 3), *Pros. priscus* (Arnaudo & Arnal 2023, figs 4.1, 4.3), *Neor. australis* (Ferreira *et al.* 2020, fig. S8) and *Do. minuscula* (Dozo 1997a, fig. 1). The paramedian fissure is visible only caudally in *Lago. maximus* (Fig. 2D) and *Di. branickii* (Ferreira *et al.* 2020, fig. S7). The preservation of *Neoe. acreensis* prevents us from making comparisons for this feature. The petrosal lobules are bulbous in *I. bolivianus*, *Lagi. peruanum*, *C. lanigera* (Figs 2, 3) and *Pros. priscus* (Arnaudo & Arnal 2023, fig. 4.3), while these structures are conical in *Lago. maximus* (Figs 2, 3). The petrosal lobules appear

distorted in *Neor. australis*, which prevents us from commenting on their shape (Ferreira *et al.* 2020, fig. S8). Despite good preservation, they are absent in *Neoe. acreensis*, and *Di. branickii* (Ferreira *et al.* 2020, figs S2, S7). Cerebellar fissures are present in *Lagi. peruanum*, *C. lanigera* and *Do. minuscula* (Dozo 1997a, fig. 1), but are absent in other specimens including *I. bolivianus* (Fig. 2). The cerebellum is not sufficiently well-preserved in the remaining natural endocasts to make comparisons, and the petrosal lobules are not visible in any of the same endocasts.

Cranial nerves & blood vessels. The casts of cranial nerves and some vessels can be seen on the ventral and lateral surfaces of the endocasts. The casts for the optic nerves (cranial nerve II) are preserved in *I. bolivianus* (Fig. 4A), and held a similar position as in all other compared taxa, being anterior to the sphenoidal fissure (Fig. 4B–D; Ferreira *et al.* 2020, figs S2, S8, S7; Arnaudo & Arnal 2023, fig. 4.2). The ancestral condition for eutherians and placental mammals probably corresponds to having the ophthalmic veins and cranial nerves III (oculomotor), IV (trochlear), V_1 (ophthalmic), V_2 (maxillary) and VI (abducens) exiting through the sphenoidal fissure. This is seen in many placental mammalian orders (e.g. dermopterans, chiropterans, carnivorans; Novacek 1986; O'Leary *et al.* 2013). This condition appears to apply to *I. bolivianus* (Fig. 4A), based on the absence of casts for any separate pathways (e.g. no sign of a distinct foramen rotundum). Positioned posteriorly, the mandibular branch of nerve V_3 would have passed through the foramen ovale in *I. bolivianus* (Fig. 4A). Two branches of V_3, the masseteric and the buccinatory nerves, would have exited the cranium through a united foramen in *I. bolivianus* located lateral to the sphenoidal fissure and oriented anterolaterally (Fig. 4A). The casts of the internal acoustic meatus with passageways for cranial nerves VII (facial) and VIII (vestibulocochlear) are located anteromedially to the petrosal lobules in *I. bolivianus* (Fig. 4A). The cast of the jugular foramen, corresponding to the passageway of the internal jugular vein and cranial nerves IX (glossopharyngeal), X (vagus), and XI (accessory) is located posterior to the internal acoustic meatus and medial to the petrosal lobules in *I. bolivianus* (Fig. 4A). The pathways of the cranial nerves would have a similar position in other compared taxa (Fig. 4B–D; Ferreira *et al.* 2020, figs S2, S8, S7; Arnaudo & Arnal 2023, fig. 4.2). The hypoglossal foramen for cranial nerve XII (hypoglossal) is not visible in *I. bolivianus* because of a lack of preservation of this area. This foramen is located posterior to the jugular foramen in *Lagi. peruanum*, *C. lanigera* and *Lago. maximus* (Fig. 4B–D), and in previously described caviomorphs (Ferreira *et al.* 2020, figs S2, S8, S7; Arnaudo & Arnal 2023, fig. 4.2).

Details of the venous drainage system can be observed in *I. bolivianus*. In dorsal view, the superior sagittal sinus is preserved and separates the cerebral hemispheres by running between them anteroposteriorly (Fig. 2A). The superior sagittal sinus would have been connected to the confluence of sinuses, which is visible in *I. bolivianus*, framing the exposed portion of midbrain medially in dorsal view (Fig. 2A). The transverse sinuses connected to the confluence of sinuses can also be observed in *I. bolivianus*, running mediolaterally along the caudal aspect of the cerebrum (Fig. 2A). In *I. bolivianus* the transverse sinus divides into two vessels: the sigmoid sinus and the capsuloparietal emissary vein (which exits the cranium as the postglenoid vein; Fig. 3A), as described in *Paramys delicatus* (Wible & Shelley 2020). In mammals, the sigmoid sinus typically runs anteroposteriorly on the lateral side of the lateral lobes of the cerebellum and then along the cerebellum ventroposteriorly to exit the cranium via the jugular foramen as the internal jugular vein (Wible 1990). Because of uneven preservation in *I. bolivianus*, we were partially able to reconstruct the sigmoid sinus, and its connection to the transverse sinus cannot be identified (Fig. S3). The CT data indicate that there might be a connection between the sigmoid sinus and capsuloparietal emissary vein via a vein, which is not sufficiently well-preserved to be reconstructed with certainty. The capsuloparietal emissary vein can be reconstructed and is connected to the transverse sinus, becoming the postglenoid vein as it exits through the postglenoid foramen (Figs 3A, S3). In *Lagi. peruanum* a similar configuration is present for capsuloparietal emissary vein. The sigmoid sinus connection with the transverse sinus is not clearly defined on the endocranial surface (Fig. S3). Additionally, as suggested for *I. bolivianus*, the sigmoid sinus is linked to the capsuloparietal emissary vein via another vein that, to our knowledge, has not been described before (Figs 3C, S3). In *C. lanigera*, a sigmoid sinus can be reconstructed, and its connection to the transverse sinus appears to run along the paramedian fissure (Fig. S3). The capsuloparietal emissary vein in *C. lanigera* appears to run along the posterior aspect of the cerebrum (connected to the endocranial cavity) from the transverse sinus to the postglenoid foramen (Figs 3B, S3). For *Lago. maximus*, the configuration is similar to *C. lanigera* for the capsuloparietal emissary vein, running along the cerebrum posteriorly, connecting the postglenoid foramen to the transverse sinus (Figs 3D, S3). However, the sigmoid sinus is not clearly identifiable on the endocranial surface (Fig. 3D). Although not labelled in *Pro. priscus*, the sigmoid sinus is visible on the endocranial surface of this specimen (Arnaudo & Arnal 2023, fig. 4). *Prospaniomys priscus* was described as having a sinus (si2), which could potentially represent a vein connecting the sigmoid sinus

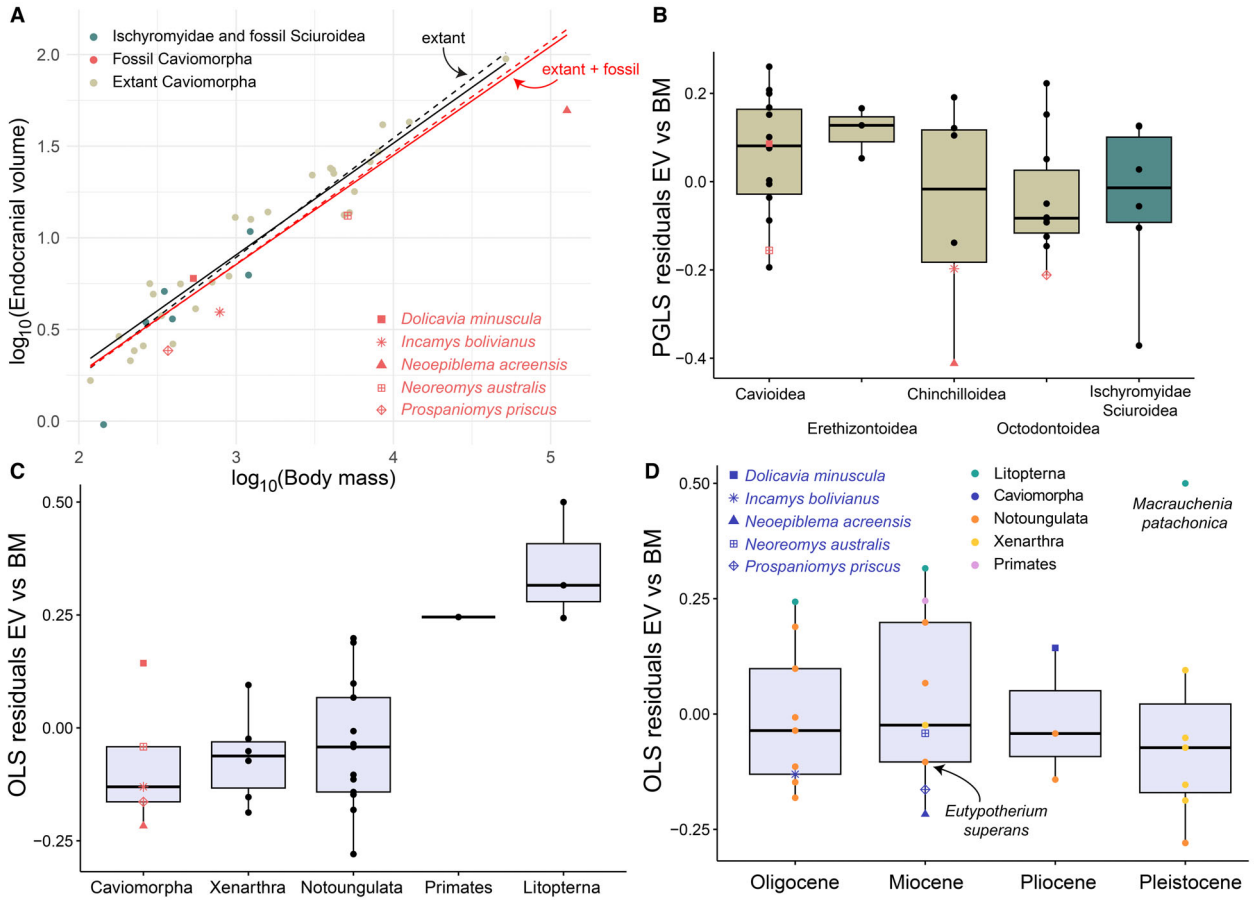

FIG. 5. Relative size of the brain of Caviomorpha and South American fossil mammals. A, linear regression of $\log_{10}$(endocranial volume) vs $\log_{10}$(body mass) for fossil and extant Caviomorpha and fossil Ischyromyidae and Sciuroidea. B, boxplot of the residuals from the phylogenetic generalized least squares (PGLS) equation in A, based on extant and fossil Caviomorpha (red solid line). C–D, boxplots of the residuals from the equation in Figure S4A, B based on an ordinary least squares (OLS) regression for all South American mammals organized by taxonomy and through time and taxonomy, respectively. In the boxplots the horizontal line represents the median, the ends of each box represent the IQR (i.e. Q1 to Q3), and the whiskers represent the minimum (Q1 − 1.5 × IQR) and maximum (Q3 + 1.5 × IQR). Black regression lines are extant Caviomorpha only; red regression lines are based on extant and fossil Caviomorpha; dashed lines are OLS; solid lines are PGLS regressions; volumetric measurements are in cm^3 and body mass was measured in g. *Abbreviations*: BM, body mass; EV, endocranial volume; IQR, interquartile range; Q, quartile.

and the capsuloparietal emissary vein (described as in part 'si1') as in the above taxa, the latter being connected to the postglenoid foramen (Arnaudo & Arnal 2023, fig. 4). The configuration of the venous system has not been described for other virtual and natural endocasts. The orbitotemporal canal is absent in *I. bolivianus* and other compared taxa.

In terms of the arterial system, extant caviomorphs appear to lack an internal carotid system. In the case of modern Chinchillidae, the blood supply of the brain is entirely assumed by the vertebral–basilar arterial system, and the external carotid system assumes the role of the stapedial artery, a branch of the internal carotid artery, which is absent in this group (Bugge 1974, 1985; Pacheco de Araújo & Campos 2005). Patterson & Wood (1982) described a potential opening anterior to the jugular foramen on the cranium of *I. bolivianus*. However, they expressed doubt about the existence of this opening and its content, which could have been arterial or venous. The CT data do not indicate any additional foramina, which instead suggests damage on the cranium. Therefore, *Incamys bolivianus* as in other caviomorph rodents lacked an internal carotid system and the brain would have been supplied by the vertebral–basilar arterial system. The endocast of *C. lanigera* has raised structures, which probably represent casts of the vertebral and basilar arteries (Fig. 4B) because they hold a similar position to those structures on the brain of a specimen of *C. lanigera* published by Pacheco de Araújo & Campos (2005, fig. 4). Pathways for the internal carotid and stapedial arteries were also not found in the specimen of *Pros. priscus* (Arnaudo & Arnal 2023). The arterial system was not

discussed for *Neor. australis*, *Neoe. acreensis* or *Di. branickii* in Ferreira *et al.* (2020). None of the nerve and vessel casts is visible in the published natural endocasts. Finally, in dorsal view, small meningeal vessels are present on the lateral surface of the cerebral hemispheres in *C. lanigera*, *Lagi. peruanum* and *Lago. maximus* (Fig. 2B–D), but are not visible in *I. bolivianus*, which could be to preservation (Fig. 2A).

Relative endocranial size. All fossil caviomorphs are below the OLS and PGLS regression lines for extant caviomorph rodents and for the entire sample except for the youngest fossil, *Do. minuscula*, which is above the lines. The PGLS regression line for extant caviomorphs has a higher intercept than, but a similar slope to, the line based on the full sample (Fig. 5A), due to the fact that the majority of fossils caviomorphs have a relatively smaller endocranial volume than extant taxa. We also note that in the North American sample (i.e. Ischyromyidae and fossil Sciuroidea), only *Prot.* cf. *rachelea* and *Miopetaurista crusafonti* are above all regression lines (Fig. 5A).

Regarding the residual values extracted from the PGLS regression of the entire rodent sample (including fossil taxa), *I. bolivianus* has a value similar to all other fossil caviomorphs except the giant rodent *Neoe. acreensis*, which has the lowest value of our rodent sample, and the youngest taxon, *Do. minuscula*, which has the highest (Fig. 5B). *Incamys bolivianus* has a smaller relative endocranial volume compared with all fossil Sciuroidea and *I. typus* except *Prosciurus relictus*, which has the lowest value for any studied taxon (except *Neoe. acreensis*; Fig. 5B). Finally, *I. bolivianus* has a smaller relative endocranial volume than all extant Chinchilloidea and Erethizontoidea, but is in the lower part of the extant range for Cavioidea and Octodontoidea (Fig. 5B).

Among the fossil mammals dating from the Oligocene to the Pleistocene of South America for which we have data, Caviomorpha, Xenarthra and Notoungulata overlap in terms of their relative endocranial volume. The primate *Chilecebus* and Litopterna have a significantly larger endocranial volume relative to body mass compared with Caviomorpha ($p = 0.043$), Xenarthra ($p = 0.034$) and Notoungulata ($p = 0.021$; Fig. 5C; Table S6). When organizing the data through time and taxonomy, all epochs overlap and no clear temporal trend can be observed (Figs 5D, S4A, B; Table S6), however, this result should be interpreted with caution because it could be due to our small and unevenly taxonomically distributed sample of endocranial data for this time range.

Olfactory bulb size. *Incamys bolivianus* and *Neor. australis* are above both the PGLS and OLS regressions with and without fossils, while *Pros. priscus* is below them (Fig. 6A). The PGLS regression lines with and without fossils have higher slope values than both OLS regressions (Fig. 6A; Table S3). *Incamys bolivianus* has the highest residual value for the relationship between the olfactory bulb volume and endocranial volume among all fossil rodents, and for all Chinchilloidea. However, *I. bolivianus* has a value close to the fossil squirrel *Prot.* cf. *rachelae* (Fig. 6B). *Incamys bolivianus* overlaps with the upper part of the range of variation of Cavioidea and Octodontoidea, while having a higher residual value than Erethizontoidea (Fig. 6B). Caviomorpha, Xenarthra and Notoungulata all have relatively larger olfactory bulbs compared with the primate *Chilecebus*. In particular, *I. bolivianus* has the highest residual values for all South American fossil mammals, indicating that it had the largest olfactory bulbs relative to endocranial volume in this group (Fig. 6C).

The PGLS and OLS regression lines for the relationship between olfactory bulb volume and body mass are relatively similar in terms of their slope and intercept (Table S3). *Incamys bolivianus* is the fossil caviomorph that is the closest to the regression lines, while *Pros. priscus* and *Neor. australis* are further below. All three fossils are below the regression lines (Fig. 6D). Regarding the residuals between olfactory bulb volume and body mass, *I. bolivianus* is near the median calculated for Chinchilloidea and overlies the value for *C. lanigera*. *Incamys bolivianus* overlaps with all other compared groups, being close to their median values, except for Erethizontoidea, compared with which it is in the upper range of variation (Fig. 6E). For the fossil taxa, Caviomorpha, Xenarthra and Notoungulata all have larger olfactory bulbs relative to body mass compared with the primate *Chilecebus*. *Incamys bolivianus* has slightly smaller olfactory bulbs relative to body mass compared with the Xenarthra *Pampatherium humboldtii*, which has the highest value for South American mammals, while the other two caviomorphs *Pros. priscus* and *Neor. australis* have lower values and overlap with each other (Figs 6F, S4C, D).

Petrosal lobule size. The PGLS and OLS regression lines for the extant sample are not significant for either the slope or the intercept (Table S3). Therefore, there is no need to correct for endocranial volume or body mass to interpret the size of the petrosal lobules because these two variables do not have an impact on the petrosal lobule size (Fig. S5). *Incamys bolivianus* falls in the range of Chinchilloidea, Cavioidea and North American rodents in term of the size of its petrosal lobules. However, *I. bolivianus* has larger petrosal lobules compared with Erethizontoidea and Octodontoidea (Fig. 7A). Erethizontoidea have significantly smaller petrosal lobules compared with Cavioidea ($p = 0.016$), and Ischyromyidae/Sciuroidea ($p = 0.043$). Octodontoidea have smaller

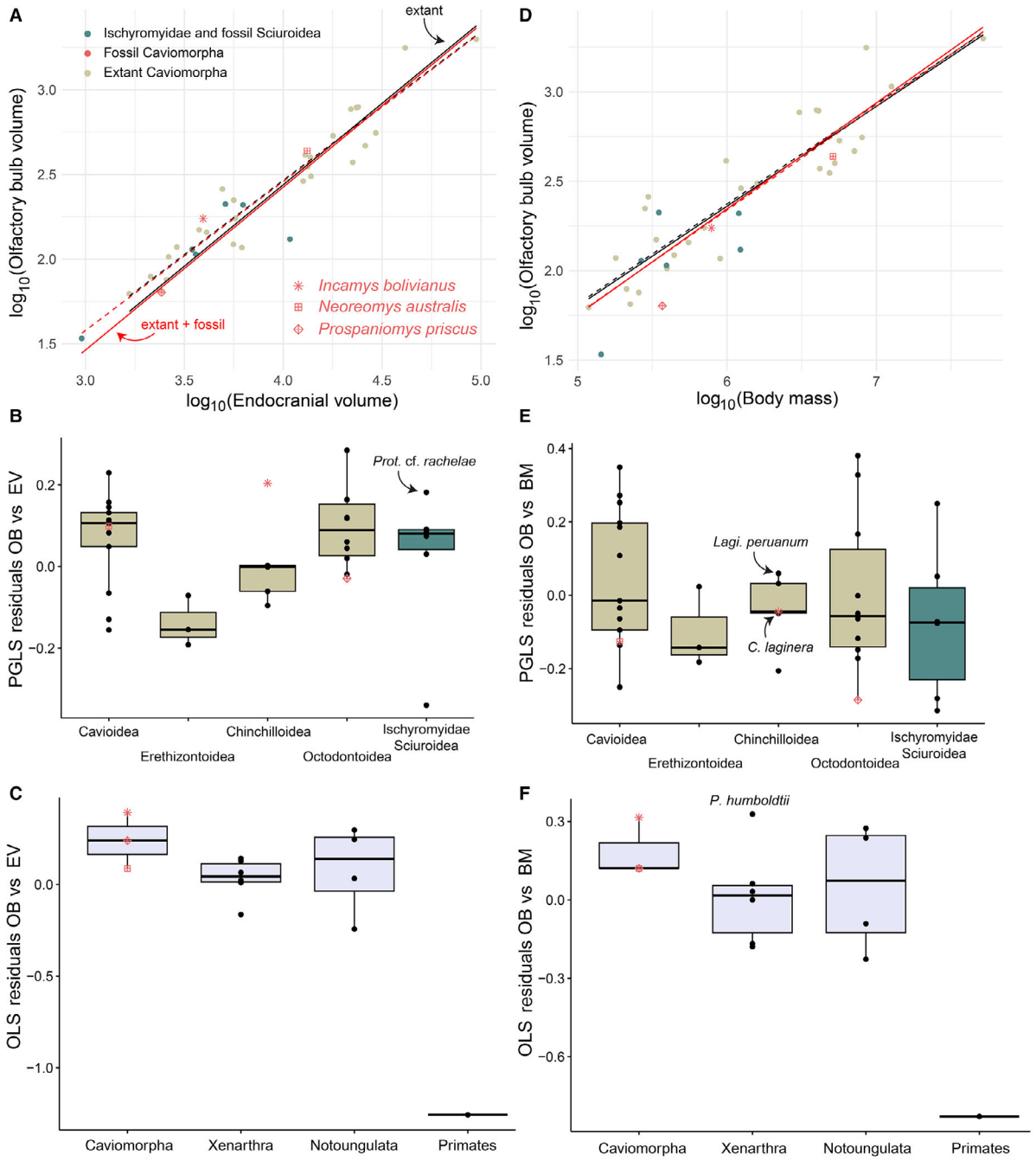

FIG. 6. Size of the olfactory bulbs relative to the endocranial volume and body mass of Caviomorpha and South American fossil mammals. A, linear regression of $\log_{10}$(olfactory bulb volume) vs $\log_{10}$(endocranial volume) for fossil and extant Caviomorpha and fossil Ischyromyidae and Sciuroidea. B, boxplot of the residuals from the phylogenetic generalized least squares (PGLS) equation in A, based on extant and fossil Caviomorpha (red solid line). C, boxplot of the residuals from the equation in Figure S4C based on an ordinary least squares (OLS) regression for all South American mammals. D, linear regression of $\log_{10}$(olfactory bulb volume area) vs $\log_{10}$(body mass) for extant and fossil Caviomorpha and fossil Ischyromyidae and Sciuroidea. E, boxplot of the residuals from the PGLS equation in D, based on extant and fossil Caviomorpha (red solid line). F, boxplot of the residuals from the equation in Figure S4D based on an OLS regression for all South American mammals. In the boxplots the horizontal line represents the median, the ends of each box represent the IQR (i.e. Q1 to Q3), and the whiskers represent the minimum (Q1 − 1.5 × IQR) and maximum (Q3 + 1.5 × IQR). Black regression lines are extant Caviomorpha only; red regression lines are based on extant and fossil Caviomorpha; dashed lines are OLS; solid lines are PGLS regressions; volumetric measurements are in mm^3 and body mass was measured in mg. *Abbreviations*: BM, body mass; EV, endocranial volume; IQR, interquartile range; OB, olfactory bulb volume; Q, quartile.

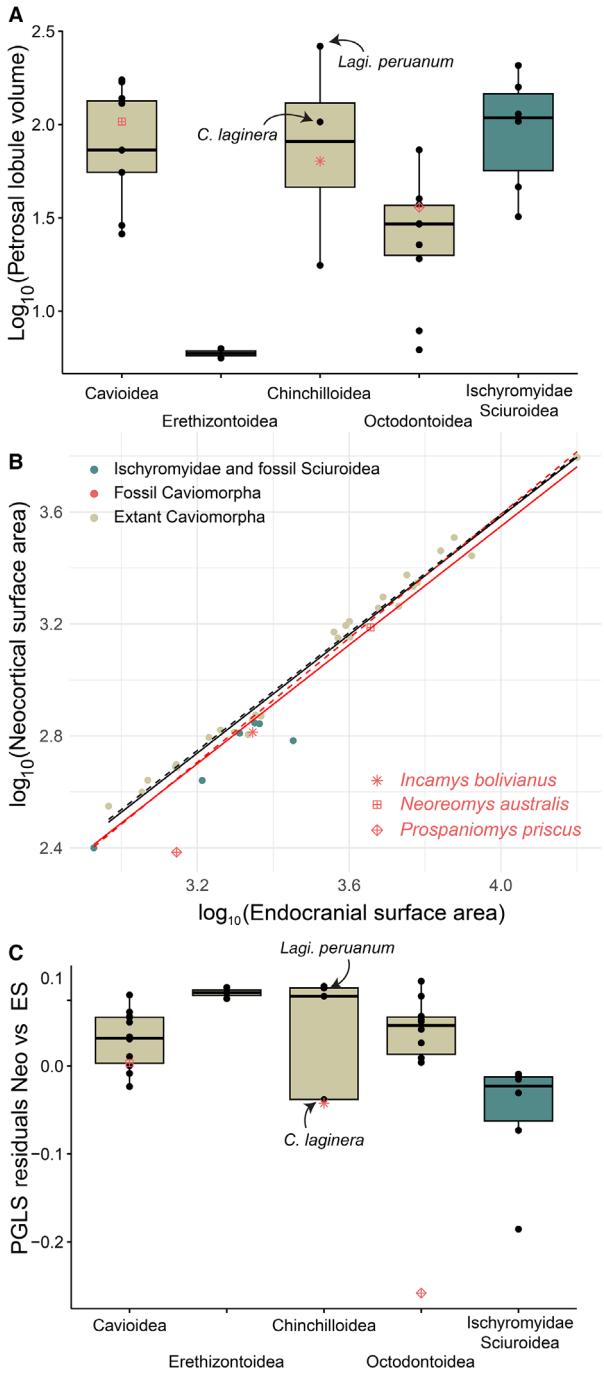

FIG. 7. Petrosal lobule size and neocortical size relative to endocranial surface area of Caviomorpha, Ischyromyidae and fossil Sciuroidea. A, boxplot of the $\log_{10}$(petrosal lobule volume). B, linear regression of $\log_{10}$(neocortical surface area) vs $\log_{10}$(endocranial surface area) for Caviomorpha and fossil Ischyromyidae and Sciuroidea. C, boxplot of the residuals from the equation in B, for the same groups based on the phylogenetic generalized least squares (PGLS) regression. In the boxplots the horizontal line represents the median, the ends of each box represent the IQR (i.e. Q1 to Q3), and the whiskers represent the minimum (Q1 − 1.5 × IQR) and maximum (Q3 + 1.5 × IQR). Black regression lines are extant Caviomorpha only; red regression lines are based on extant and fossil Caviomorpha; dashed lines are ordinary least squares (OLS); solid lines are PGLS regressions; volumetric measurements are in mm^3; surface area measurements are in mm^2. *Abbreviations*: ES, endocranial surface area; IQR, interquartile range; Neo, neocortical surface area; Q, quartile.

petrosal lobules compared with Cavioidea ($p = 0.016$), and Ischyromyidae/Sciuroidea ($p = 0.028$; Fig. 7A; Table S5).

Neocortical size. An almost isometric linear relationship is present between the neocortical surface area and the endocranial surface area in our sample (Tables S3, S4). *Incamys bolivianus* and *Pros. priscus* are below both OLS and PGLS regressions for both the analysis based on the extant sample only and on the analysis including the fossils, while *Neor. australis* sits on the PGLS regression line in the analysis including the fossils, and is only very slightly below the other calculated lines (Fig. 7B). *Incamys bolivianus* has a residual value close to the extant chinchillid *C. lanigera*, has a lower value compared with *Neor. australis* but higher than *Pros. priscus*, which has the lowest value of the sample (Fig. 7C). *Incamys bolivianus* has a lower residual value than *Lagi. peruanum*, and *Lago. maximus*, Cavioidea, Erethizontoidea, Octodontoidea, but overlaps with fossil Ischyromyidae/Sciuroidea. None of the groups is significantly different (Fig. 7C; Table S5).

Incamys bolivianus, *Neor. australis* and the Notoungulata *Mesotherium maendrum* (MACN PV 2925) are above the OLS regression line for the South American fossil sample (Fig. S6A). The neocortical residual values for *I. bolivianus* and *Neor. australis* are higher than for Notoungulata and *Pros. priscus* (Fig. S6B).

DISCUSSION

Inferred ancestral endocranial brain morphology of Caviomorpha

Arnaudo & Arnal (2023) described the 'rhomboidal' morphology related to the lateral extension of the temporal lobes in the Early Miocene pan-octodontoid, *Pros. priscus*, which they found was somewhat similar to the extant Chinchillidae, *Chinchilla*. The late Oligocene stem chinchillid *I. bolivianus* shows even more extended temporal lobes, similar to extant Chinchillidae, in contrast to the Pan-Octodontoidea *Pros. priscus* and *Me. primitiva*. This could suggest that by the late Oligocene, Chinchillidae were already characterized by this temporal expansion of

the cerebrum. As mentioned by Arnaudo & Arnal (2023), this characteristic is also present in the natural endocast of the Miocene 'Cephalomyidae' gen. et sp. indet. described by Dozo (1997b). This particular shape was hypothesized to potentially represent a shared feature between Chinchillidae and the 'Cephalomyidae' (Dozo 1997b), which has been found as a potential close relative to modern Chinchillidae based on dental features (Rasia & Candela 2019). The other extant Chinchilloidea clade, Dinomyidae, shows a slightly different cerebral shape with a cerebrum more convex anteriorly, without any marked concavity, compared with Chinchillidae and Cephalomyidae. It is possible that the condition in the extant *Di. branickii* is a derived feature and that the ancestral condition for Chinchilloidea as a whole was more similar to *I. bolivianus*. The condition is unclear for the Neoepiblemidae *Neoe. acreensis* closely related to 'Cephalomyidae' (Rasia & Candela 2019), because of the distortion present in the specimen (Ferreira *et al.* 2020, fig. S2). The natural endocast of *Hypsosteiromys* already shows a similar condition to modern erethizontids in which the cerebrum is wider anteriorly (Dozo *et al.* 2004). We suspect that this condition might be derived in this group. It is worth noting that modern Cavioidea and the fossil *Neor. australis* and *Do. minuscula* also have this type of temporal extension (Ferreira *et al.* 2020, 2022), therefore this feature could have potentially been shared by the common ancestor of Caviomorpha as suggested by Arnaudo & Arnal (2023); however, older fossils for the various caviomorph clades will be required to test this hypothesis regarding the utility of this anatomical feature in resolving the phylogenetic relationships of Caviomorpha.

The neocortex is the region of the brain associated with the integration of sensory and motor functions and manages vision, hearing, motor skills, high-level cognition, and memory (Jerison 1973; Christensen & Evans 1979; Kaas 2020). Increases in neocortical size occurred in placental mammals from the Paleocene to the Eocene and during the Eocene, and placental crown clades also have more expanded neocortices than archaic placental mammals (Bertrand *et al.* 2022 and references therein). In keeping with this observation, the rodent crown clade Sciuroidea shows an increase in neocortical size compared with the 'archaic' rodent group, Ischyromyidae, during the early Oligocene (Bertrand *et al.* 2017, 2018). The results from *I. bolivianus* indicate that by the late Oligocene, the neocortical size of Caviomorpha had reached similar levels to those of Sciuroidea. In order to have a better understanding of the ancestral condition of Caviomorpha, the inclusion of Eocene Hystricognati or Ctenohystrica would be ideal; however, no virtual endocasts of either of the clades have been described so far. The early Glires *Rhombomylus* can be considered to show the ancestral condition for rodents and has a relatively small neocortex (Meng *et al.* 2003, fig. 50). Modern Caviomorpha and Sciuroidea have relatively large neocortices. The closest relatives of Sciuroidea, Ischyromyidae, had smaller neocortices than the modern clade, but bigger than *Rhombomylus*. This would suggest an independent increase in neocortical size in two distantly related lineages of rodents (i.e. Sciuroidea and Caviomorpha). If there was only one increase event in neocortical size, then Ischyromyidae would have had to have an equivalent neocortical size to squirrels and caviomorphs. Interestingly, the neocortical size of the Miocene pan-Octodontoidea *Pros. priscus* is lower than that for *I. bolivianus* (at the level of Eocene Ischyromyidae; Arnaudo & Arnal 2023), which could potentially represent an ancestral trait or a specialization to a specific lifestyle. As a result, the condition of the common ancestor for Caviomorpha remains equivocal, and earlier occurring fossils will be needed.

A lissencephalic neocortex is considered the ancestral condition for rodents based on fossil Glires (Meng *et al.* 2003), but also for mammals based on Mesozoic fossils (Rowe *et al.* 2011). There is also a correlation between brain size and gyrencephalization in extant species (Macrini *et al.* 2007). Extant rodents can have either lissencephalic or gyrencephalic brains. Brains of extant species with either of these two states are found throughout a brain size ranging from 3 to 30 cm^3 (Pilleri *et al.* 1984). All early rodents in the family Ischyromyidae are found within the range of this extant rodent sample and the majority of fossil ischyromyids have lateral sulci (Bertrand *et al.* 2019). *Incamys bolivianus* is in the low range with a brain size of 4 cm^3 and presents lateral sulci, which suggests some folding of the brain. Interestingly, the Miocene pan-Octodontoidea *Pros. priscus* has lateral sulci but is below the Pilleri *et al.* (1984) range with a brain size of only 2.4 cm^3 (Arnaudo & Arnal 2023). This suggests that the common ancestor of Caviomorpha probably had a small brain that was either lissencephalic or with lateral sulci and therefore some potentially limited brain folding.

Midbrain exposure and enhanced auditory acuity

Exposure of the midbrain has often been interpreted as a plesiomorphic feature for mammals associated with limited expansion of the neocortex. Indeed, midbrain exposure is visible in fossil mammals from distinct lineages including 'plesiadapiform' primates (Silcox *et al.* 2009, 2010; Orliac *et al.* 2014; White *et al.* 2023), early glirans, rodents and lagomorphs (Bertrand *et al.* 2016b, 2017, 2019; Meng *et al.* 2003; López-Torres *et al.* 2020), bats (Maugoust & Orliac 2021), artiodactyls (Orliac &

Gilissen 2012), and 'condylarths' (Orliac *et al.* 2012). Concerning caviomorph rodents more specifically, the midbrain may have been exposed in the 'Cephalomyidae' gen. et. sp. indet. described by Dozo (1997b), but it remains ambiguous based on the preservation. The same is true for the natural endocast of *Me. primitiva* (Piñero *et al.* 2021). The midbrain is exposed in the virtual endocast of *Pros. priscus* (Arnaudo & Arnal 2023). Besides these three specimens, the midbrain is not exposed in any of the other fossil specimens or in extant caviomorph rodents.

Some extinct mammals have a more complex midbrain morphology with exposed caudal colliculi (= inferior colliculi) that are related to acoustic reflexes (Christensen & Evans 1979), including but not limited to the Eocene 'condylarth' *Hyopsodus* (Orliac *et al.* 2012) and bat *Palaeophyllophora* (Maugoust & Orliac 2021), as well as the rodents *Reithroparamys* and *Ischyromys* (Bertrand & Silcox 2016; Bertrand *et al.* 2019; Bertrand & Silcox 2023). Extensive midbrain exposure with visible caudal colliculi has been viewed as potentially being a derived characteristic that could be linked to enhanced auditory acuity (Edinger 1964). *Incamys bolivianus* is the oldest caviomorph to date and the only caviomorph rodent with a clearly exposed midbrain including visible caudal colliculi. This suggests that the ancestor of Chinchillidae and possibly Caviomorpha had an exposed midbrain. However, the presence of the caudal colliculi could be related to enhanced auditory capabilities in *I. bolivianus* and be considered a derived feature shared with extant Chinchillidae. The midbrain is covered by the cerebrum and cerebellum in *Chinchilla* and *Lagostomus*. However, thin sections through the brain (Brauer & Schober 1970; Harrison *et al.* 1998; D'Alessandro & Harrison 2016) show that the caudal colliculi are physically large compared with the rostral colliculi (= superior colliculi; related to vision; Christensen & Evans 1979). The caudal colliculi are usually located ventral to the rostral colliculi, but in these taxa the caudal colliculi are so large that they come into contact with the cerebrum or the cerebellum dorsally. In contrast, in *Sciurus vulgaris* they are positioned ventral to the rostral colliculi (Brauer & Schober 1970). In the latter, larger rostral colliculi might be associated with enhanced visual acuity, as shown for treeshrews (Petry & Bickford 2019). During the late Oligocene, the caudal colliculi may have had an important role in auditory function in *Incamys*. Modern chinchillids are very social animals that communicate via different calls. Specifically, *Chinchillas* have four types of vocalizations (Francescoli *et al.* 2016). In rodents, including *Chinchillas*, the caudal colliculi are crucial for processing vocalization within a species (Klepper & Herbert 1991; Portfors & Sinex 2005; Petersen & Hurley 2017). Additionally, the auditory cortex is located in the temporal lobe of the neocortex (Krubitzer *et al.* 2011). Given that the temporal lobes are laterally extended in Chinchillidae and *Incamys* (see discussion above), this could also reflect enhanced auditory capabilities.

The social complexity hypothesis for communication (SCHC) proposes that larger groups of individuals require a more complex set of social interactions (Freeberg *et al.* 2012). For example, the SCHC has been verified for the caviomorph *Cuniculus paca*, which has seven vocal types and lives in groups in captivity (Lima *et al.* 2018). Additionally, a recent study showed that for extant caviomorph rodents, group-living was reconstructed as the ancestral state for this clade (Sobrero *et al.* 2014). This could therefore potentially represent the first evidence that by the late Oligocene, Chinchillidae already lived in groups and used vocalizations to communicate with each other. To our knowledge, this would be the first time that a brain endocranial attribute (i.e. caudal colliculi), apart from the relative size of the brain and neocortex (Shultz & Dunbar 2006) has been used as evidence of social complexity in the fossil record. Alternatively, enhanced audition could have been used in another setting other than living in a group, such as having first evolved to find mates (Charlton & Reby 2016), and was later used in modern species to communicate with members of a group for reasons such as predator avoidance.

Sensory ecology in Caviomorpha

The proportion of different brain regions can be compared by studying the relationship between the volume of these regions and overall brain volume. The olfactory bulbs are relatively smaller in squirrels than in ischyromyids, but their size relative to body mass appears to be equivalent in the two groups, suggesting that other parts of the brain, such as the neocortex and the petrosal lobules, were expanded in fossil squirrels compared with Ischyromyidae (Bertrand & Silcox 2023). This suggests that olfaction might have remained constant through time in squirrels (and not decreased). In addition to olfaction, other senses may have emerged with the expansion of the neocortex and petrosal lobules. In Chinchillidae, *I. bolivianus* has larger olfactory bulbs relative to endocranial volume than in extant taxa, but the relationship to body mass is similar to that in extant species, which is similar to the condition in squirrels (Fig. 6). Therefore, a similar conclusion can be reached for Chinchillidae, that is, that ancestrally olfaction was a major sense used for survival at least during the Oligocene that is probably still important today. The neocortical size of *Incamys* is in the lower range of the available data for Chinchilloidea; However, it is very close to the value of the modern *Chinchilla* (Fig. 7C). These results suggest that *Chinchilla* retained

the ancestral condition for Pan-Chinchillidae for the neocortex (relative to endocranial volume) and olfactory bulbs (related to body mass). The fact that the olfactory bulbs are bigger relative to endocranial volume in *Incamys*, suggests that other brain regions have expanded from the Oligocene to today in *Chinchilla*. In this case, the petrosal lobules are bigger in *Chinchilla* than in *Incamys* (Fig. 7A). Additionally, the cerebellum shows greater complexity in the *Chinchilla*, with cerebellar fissures, compared with *Incamys* (Fig. 2), suggesting that this part of the brain increased in proportion. The other chinchillid species *Lagidium* has a different pattern with an increase in the neocortex and the petrosal lobules similar to squirrels (Fig. 7A, C). It is worth noting that the residual values from the regressions of the olfactory bulb volume versus endocranial volume and versus body mass are lower in the Miocene Octodontoidea *Pros. priscus* and Cavioidea *Neor. australis* compared with those of *I. bolivianus*. Because of this discrepancy it is challenging to estimate what the ancestral olfactory bulb size, and the size relative to other regions, would have been in early Caviomorpha. Therefore, more basal taxa are needed to help answer this question.

Concerning the neocortical size, *I. bolivianus* has a more expanded neocortex than we would expect in a fossil rodent that has exposed caudal colliculi. Indeed, the two Ischyromyidae *Reithroparamys* and *Ischyromys* have much smaller neocortical ratios (17–21%; Bertrand *et al.* 2021) compared with *I. bolivianus* (29%), which is instead more similar to the squirrel *Cedromus wilsoni* that has a covered midbrain (32%; Bertrand *et al.* 2017). It remains unclear which part of the neocortex is expanded in *I. bolivianus*, but it could potentially be the auditory cortex (lateral extension of the temporal lobes) as opposed to the visual cortex in squirrels.

The petrosal lobules have a role in maintaining eye and head movements during locomotion (Rambold *et al.* 2002). Previously, we observed an increase in petrosal lobule size that coincided with the transition to living in trees in squirrels (Bertrand *et al.* 2017, 2021). We deduced that squirrels living in the 3D complex environment of the trees require a certain amount of eye and head stabilization to rapidly navigate a cluttered space involving jumping onto small branches. We have limited data for caviomorph rodents, but the pattern observed in squirrels might be different from that which pertains to caviomorph rodents. Based on a recent study, Fernández Villoldo *et al.* (2023) found that scansorial and terrestrial species had larger petrosal lobules (i.e. residual centroid size ratio) than arboreal taxa in Echimyidae. They noted that the arboreal species slowly and carefully climb branches (Emmons 1981), while the scansorial and terrestrial species (dos Reis & Pessôa 2004; Pessôa *et al.* 2015) are more agile and would potentially require more eye and head stabilization during rapid movements. This finding confirms a major issue that still needs to be addressed, that is, the need for arboreal and more general locomotor categories that differentiate between animals with different agilities. Spoor *et al.* (2007) created a method using agility scores that classifies mammals in terms of their speed of movement rather than their locomotion. However, a lot of overlap exists between the different scores, which were defined based on video footage, and therefore represent a limitation in applying this method more broadly. It is worth acknowledging that the lack of a general pattern between ecology and petrosal lobules was found in a recent study on Euarchontoglires (Lang *et al.* 2022).

For caviomorphs, the fossil record is too poor to make a connection between petrosal lobules and locomotor behaviour. We refrain from doing an analysis based on traditional locomotor behaviours because our sample size is relatively low and the creation of new locomotor categories is beyond the scope of this paper. However, we observe that Cavioidea, which includes many cursorial species that require high agility when moving in a cluttered space, such as the genus *Dasyprota* (Elissamburu & Vizcaíno 2004; Sobrero *et al.* 2014), have large petrosal lobules. Additionally, the Chinchillidae *Chinchilla* and *Lagidium*, both considered rock-dwellers and jumpers (Elissamburu & Vizcaíno 2004; Candela *et al.* 2017), also have relatively large petrosal lobules. Erethizontoidea are arboreal (Candela *et al.* 2017), however, they include slow climbers such as *Coendou* (Griffiths *et al.* 2020) and have some of the smallest petrosal lobules of the sample. No postcrania have been recovered for *Incamys*. Considering that *I. bolivianus* has smaller petrosal lobules than the chinchillids *Chinchilla* and *Lagidium*, this Oligocene taxon may have been less agile than its extant relatives. *Incamys bolivianus* had larger petrosal lobules than the slower arboreal extant Octodontoidea and Erethizontoidea. Based on modern caviomorphs and the data currently available, we could speculate that *Incamys* was more of a ground-dweller that used fairly rapid movements, and that the common ancestor of Caviomorpha was spending more time on the ground than in the trees; however, early fossils are necessary to test this hypothesis. We note that the semicircular canals could also provide an indication of the level of agility of *Incamys*, but this is beyond the scope of this paper and will be the subject of future work.

Brain evolution of Caviomorpha and other South American mammals

South America was isolated from the rest of the world at least until the Miocene, but then, several waves of

migration occurred between South and North America in both directions, which accelerated towards the end of the Pliocene with the formation of the Isthmus of Panama (Chávez Hoffmeister 2020). This event is known as the Great American Biotic Interchange (GABI; Marshall *et al.* 1983; Stehli & Webb 1985). Therefore, prior to that point (at least until the Miocene), South America provided the mammals living there with a microworld where they could branch off onto their own evolutionary trajectories. Concerning the brain evolution of these species, endocranial data of fossils from the Oligocene to the Pleistocene show that Litopterna and Primates had bigger brains relative to body mass than Caviomorpha, Xenarthra and Notoungulata. The reason for this disparity is unclear for Litopterna. This group appears to have relatively complex brains and large neocortices that could have contributed to this relatively large brain (Dozo *et al.* 2023, fig. 21.5). This is not the first time that comparisons have been made among fossil mammals of South America. Dozo (1997a) made a comparison between the Pliocene rodent *Do. minuscula* (MMP M-1364) and the Notoungulata *Paedotherium insigne* (MMP 386-S). Interestingly, Dozo (1997a) found many convergent morphological features between the two taxa including similar neocortical sulci (i.e. lateral, suprasylvian and pseudosylvian), possibly suggesting equivalent enhanced brain functions in these two distantly related mammalian groups.

Concerning relative brain size, we have found no particular pattern through time besides a very high residual value for the Pleistocene litoptern *Ma. patachonica*. The very small amount of data do not enable us to test whether this value could be related to competition with North American taxa that immigrated to South America. This overall pattern contrasts with mammals in general (Jerison 1973; Bertrand *et al.* 2022); however, this could be due to the small sample size and the fact that our sample distribution is skewed because it relies on the availability of endocranial data for fossils. Bertrand *et al.* (2022) found that the increase in relative brain size from the Paleocene to the Eocene was due to a major increase in the neocortical size for a large sample of placental mammals. Nevertheless, this hypothesis has never been tested beyond the Oligocene in North American mammals and the data were very limited for this epoch (Jerison 1961). For South America, Fernández-Monescillo *et al.* (2019) did not find a noticeable relative brain size increase in Notoungulata from the Oligocene to the Miocene. In the future it would be interesting to investigate the differences in relative brain size and regions of the brain between South and North American taxa during these different epochs to evaluate the role of the neurosensory system in the extinction of Notoungulata and Litopterna. For rodents in North America specifically, no temporal effect was found, but the data are again relatively limited (Bertrand *et al.* 2019).

In terms of the relative size of the neocortex, the data are scarce but *Neor. australis* and *I. bolivianus* both have higher residual values than Notoungulata (Fig. S5B). This fact is interesting because some notoungulates (i.e. *Rhynchippus equinus*, *Mesotherium maendrum*, *Mendozahippus fierensis* and *Nesodon imbricatus*) have a higher number of sulci on their neocortices (Dozo & Martínez 2016; Fernández-Monescillo *et al.* 2019; Martínez *et al.* 2019, 2023) than *I. bolivianus* and *Neor. australis* but lower neocortical residual values. This discrepancy could be related to the fact that notoungulates are much larger than rodents therefore they require larger brains, which may become more gyrencephalic for packing reasons rather than because the neocortex is relatively large. It is also possible that the neocortical surface area of notoungulates is underestimated because part of the neocortex is folded.

CONCLUSION

Our study focuses on describing the oldest brain endocast for a caviomorph rodent, the stem Pan-chinchillid *I. bolivianus*. This taxon has features that could be considered ancestral for Chinchillidae as well as for Caviomorpha as a whole, although this is a hypothesis that will need to be tested with additional fossil endocasts. By the late Oligocene caviomorphs had a temporal extension of the cerebrum, and had independently reached a neocortical size similar to that of contemporaneous squirrels from North America. The ancestor of caviomorph rodents probably had a lissencephalic brain or at most had a few sulci, and an exposed midbrain.

This combination of an extended temporal lobe of the neocortex and exposed caudal colliculi is unique so far for fossil rodents. Based on the fossil record, the expansion of the neocortex caudally in squirrels has been hypothesized to be related to the expansion of the occipital lobe where the visual cortex is located (Bertrand *et al.* 2017). In contrast to squirrels that rely heavily on vision, it is possible that *Incamys* relied more heavily on hearing because of the lateral extension of the neocortex (location of the auditory cortex) and its potentially large caudal colliculi associated with better sound processing. Modern chinchillids live in colonies and communicate among members of a group using various calls (Francescoli *et al.* 2016), and caudal colliculi have a role in processing vocalization (Klepper & Herbert 1991; Petersen & Hurley 2017). Therefore, this pattern observed in *Incamys* could be the first evidence of complex communication based on an endocranial structure, apart from the relative size of the brain and neocortex (Shultz & Dunbar 2006). However,

enhanced audition could have evolved for other reasons that are not specific to group-living such as finding a mate (Charlton & Reby 2016).

The role of the olfactory bulbs would have probably been more crucial for survival in the early evolution of Chinchillidae and possibly more broadly in Caviomorpha and then was assisted by the expansion of the neocortex in extant species, except for *Chinchilla*, in which it would have been related to cerebellar increase only. *Incamys bolivianus* was probably less agile than modern chinchillids as suggested by its smaller petrosal lobules, which are not as reduced as in slow arboreal porcupines. Current neurosensory data are compatible with a ground-dwelling lifestyle possibly using fairly rapid locomotion.

Variation in relative brain size is observed for different South American mammalian clades from the Oligocene to the Pleistocene. The absence of a temporal effect on relative brain size could be due to sample size and taxonomic distribution. Caviomorpha are in the range of Notoungulata and Xenarthra in terms of relative brain size. However, *Incamys* and *Neoreomys* both have higher neocortical surface area residuals than Notoungulata. Knowing that the neocortex of Notoungulata has many more sulci, it is possible that the neocortical size of Notoungulata is underestimated because of the folding of this structure when its size increases.

Ultimately, additional fossils will be necessary to more fully understand how the neurosensory system of caviomorph rodents evolved, compared with other endemic South American mammals.

Acknowledgements. We would like to thank D. Brinkman, M. Fox and C. Norris from the Yale Peabody Museum for providing access to the specimen of *Incamys bolivianus*, and E. Westwig from the American Museum of Natural History (AMNH) for access to the specimens of *Chinchilla lanigera* and *Lagostomus maximus*. We also thank J. Thostenson and D.M. Boyer for facilitating the scanning of the specimen at the SMIF (Duke University), and M. Hill from the AMNH Microscopy and Imaging Facility for scanning the AMNH specimens. The generation of the virtual endocast of *C. lanigera* was part of segmentation training of undergraduate students at the University of Toronto, Scarborough, between 2013 and 2015. We would like to thank: Samantha Gionfriddo, Lavania Nagendran and Jamila Norman for their enthusiasm and hard work. This work was supported by Marie Skłodowska-Curie Actions: Individual Fellowship, H2020-MSCA-IF-2018-2020, no. 792611 (OCB); Beatriu de Pinós Programme funded by the Direcció General de Recerca de la Generalitat de Catalunya (General Directorate for Research in the Government of Catalonia) and managed by AGAUR, expedient number: 2021 BP 00042 (OCB), and CERCA Programme/Generalitat de Catalunya; NSERC Discovery Grant to MTS. There is no conflict of interest. We would like to thank J.R. Wible for fruitful discussions as well as M.E. Arnaudo, M.E. Pérez and an anonymous reviewer for their helpful suggestions and comments on the manuscript.

Author contributions. This work was originally planned to be part of the PhD dissertation of OCB at the University of Toronto under the supervision of MT Silcox. **Conceptualization** OC Bertrand (OCB); **Data Curation** OCB, MM Lang (MML), JD Ferreira (JDF), L Kerber (LK); **Formal Analysis** OCB; **Funding Acquisition** OCB, MT Silcox; **Investigation** OCB, MML, JDF, Zoi Kynigopoulou (ZK); **Methodology** OCB, MML; **Supervision** OCB, MT Silcox (MTS); **Visualization** OCB; **Writing – Original Draft Preparation** OCB; **Writing – Review & Editing** OCB, MTS, MML, ZK.

DATA ARCHIVING STATEMENT

Brain virtual endocasts for the different specimens are available in MorphoSource: https://www.morphosource.org/projects/000592514 (see also Table S2).

Editor. Kenneth Angielczyk

SUPPORTING INFORMATION

Additional Supporting Information can be found online (https://doi.org/10.1002/spp2.1562):

Fig. S1. Topology used in the PGLS equations.
Fig. S2. Virtual reconstructions in latero-dorsal view of the brain virtual endocast of the stem Chinchillidae *Incamys bolivianus* (YPM VPPU 21945).
Fig. S3. Virtual reconstructions in dorsal and lateral views of the virtual endocast of the brain, transverse and sigmoid sinuses and associated veins of *Incamys bolivianus* (YPM VPPU 21945), *Chinchilla lanigera* (AMNH 180038) and *Lagidium peruanum* (NMB 1043).
Fig. S4. Relative endocranial volume and size of the olfactory bulbs relative to endocranial volume and body mass for South American fossil mammals.
Fig. S5. Size of the petrosal lobules relative to endocranial volume and body mass of Caviomorpha, Ischyromyidae and fossil Sciuroidea.
Fig. S6. Linear regression of $\log_{10}$ (neocortical surface area vs endocranial surface area) for South American fossil mammals, and boxplot of the residuals for the same groups based on an OLS regression.
Table S1. Endocranial volume and surface area data gathered for our sample. Body mass, endocranial, olfactory bulb and petrosal lobule volumes, endocranial and neocortical surface areas for the specimens used in the different analyses.
Table S2. DOIs for data archived in MorphoSource.
Table S3. Results from the PGLS and OLS regressions for the different endocranial variables and for extant Caviomorpha and for extant + fossil Caviomorpha, Ischyoromyidae, and Sciuroidea.

Table S4. Results from the PGLS and OLS regressions for the different endocranial variables and for all South American mammals.
Table S5. Asymptotic K-sample Fisher–Pitman permutation test, and pairwise comparisons for Caviomorpha, Ischyromyidae and Sciuroidea.
Table S6. Asymptotic K-sample Fisher–Pitman permutation test, Welch test, and pairwise comparisons for all South American mammals.
Appendix S1. The R code required to reproduce the analysis.

REFERENCES

Álvarez, A. and Arnal, M. 2015. First approach to the paleobiology of extinct *Prospaniomys* (Rodentia, Hystricognathi, Octodontoidea) through head muscle reconstruction and the study of craniomandibular shape variation. *Journal of Mammalian Evolution*, **22**, 519–533.

Álvarez, A. and Ercoli, M. D. 2017. Why pacaranas never say no: analysis of the unique occipitocervical configuration of †*Tetrastylus intermedius* Rovereto, 1914, and other dinomyids (Caviomorpha; Dinomyidae). *Journal of Vertebrate Paleontology*, **37**, e1385476.

Álvarez, A., Arévalo, R. L. M. and Verzi, D. H. 2017. Diversification patterns and size evolution in caviomorph rodents. *Biological Journal of the Linnean Society*, **121**, 907–922.

Álvarez, A., Ercoli, M. D. and Verzi, D. H. 2020. Integration and diversity of the caviomorph mandible (Rodentia: Hystricomorpha): assessing the evolutionary history through fossils and ancestral shape reconstructions. *Zoological Journal of the Linnean Society*, **188**, 276–301.

Antoine, P. O., Marivaux, L., Croft, D. A., Billet, G., Ganerod, M., Jaramillo, C., Martin, T., Orliac, M. J., Tejada, J., Altamirano, A. J., Duranthon, F., Fanjat, G., Rousse, S. and Gismondi, R. S. 2012. Middle Eocene rodents from Peruvian Amazonia reveal the pattern and timing of caviomorph origins and biogeography. *Proceedings of the Royal Society B*, **279**, 1319–1326.

Arnal, M. and Vucetich, M. G. 2015. Main radiation events in Pan-Octodontoidea (Rodentia, Caviomorpha). *Zoological Journal of the Linnean Society*, **175**, 587–606.

Arnal, M., Kramarz, A. G., Vucetich, M. G., Frailey, C. D. and Campbell, K. E. Jr 2020. New Palaeogene caviomorphs (Rodentia, Hystricognathi) from Santa Rosa, Peru: systematics, biochronology, biogeography and early evolutionary trends. *Papers in Palaeontology*, **6**, 193–216.

Arnal, M., Pérez, M. E., Tejada Medina, L. M. and Campbell, K. E. 2022. The high taxonomic diversity of the Palaeogene hystricognath rodents (Caviomorpha) from Santa Rosa (Peru, South America) framed within a new geochronological context. *Historical Biology*, **34**, 2350–2373.

Arnaudo, M. E. and Arnal, M. 2023. First virtual endocast description of an early Miocene representative of Pan-Octodontoidea (Caviomorpha, Hystricognathi) and considerations on the early encephalic evolution in South American rodents. *Journal of Paleontology*, **97**, 454–476.

Bertrand, O. C. and Silcox, M. T. 2016. First virtual endocasts of a fossil rodent: *Ischyromys typus* (Ischyromyidae, Oligocene) and brain evolution in rodents. *Journal of Vertebrate Paleontology*, **36**, 1–19.

Bertrand, O. C. and Silcox, M. T. 2023. Brain evolution in fossil rodents: a starting point. 645–680. *In* Dozo, M. T., Paulina-Carabajal, A., Macrini, T. E. and Walsh, S. (eds) *Paleoneurology of amniotes: New directions in the study of fossil endocasts*. Springer, 840 pp.

Bertrand, O. C., Flynn, J. J., Croft, D. A. and Wyss, A. R. 2012. Two new taxa (Caviomorpha, Rodentia) from the Early Oligocene Tinguiririca Fauna (Chile). *American Museum Novitates*, **2012**, 1–36.

Bertrand, O. C., Schillaci, M. A. and Silcox, M. T. 2016a. Cranial dimensions as estimators of body mass and locomotor habits in extant and fossil rodents. *Journal of Vertebrate Paleontology*, **36**, e1014905.

Bertrand, O. C., Amador-Mughal, F. and Silcox, M. T. 2016b. Virtual endocasts of Eocene *Paramys* (Paramyinae): oldest endocranial record for Rodentia and early brain evolution in Euarchontoglires. *Proceedings of the Royal Society B*, **283**, 20152316.

Bertrand, O. C., Amador-Mughal, F. and Silcox, M. T. 2017. Virtual endocast of the early Oligocene *Cedromus wilsoni* (Cedromurinae) and brain evolution in squirrels. *Journal of Anatomy*, **230**, 128–151.

Bertrand, O. C., Amador-Mughal, F., Lang, M. M. and Silcox, M. T. 2018. Virtual endocasts of fossil Sciuroidea: brain size reduction in the evolution of fossoriality. *Palaeontology*, **61**, 919–948.

Bertrand, O. C., Amador-Mughal, F., Lang, M. M. and Silcox, M. T. 2019. New virtual endocasts of Eocene Ischyromyidae and their relevance in evaluating neurological changes occurring through time in Rodentia. *Journal of Mammalian Evolution*, **26**, 345–371.

Bertrand, O. C., Püschel, H. P., Schwab, J. A., Silcox, M. T. and Brusatte, S. L. 2021. The impact of locomotion on the brain evolution of squirrels and close relatives. *Communications Biology*, **4**, 460.

Bertrand, O. C., Shelley, S. L., Williamson, T. E., Wible, J. R., Chester, S. G. B., Flynn, J. J., Holbrook, L. T., Lyson, T. R., Meng, J., Miller, I. M., Püschel, H. P., Smith, T., Spaulding, M., Tseng, Z. J. and Brusatte, S. L. 2022. Brawn before brains in placental mammals after the end-Cretaceous extinction. *Science*, **376**, 80–85.

Boivin, M., Ginot, S., Marivaux, L., Altamirano-Sierra, A. J., Pujos, F., Salas-Gismondi, R., Tejada-Lara, J. V. and Antoine, P.-O. 2018. Tarsal morphology and locomotor adaptation of some late middle Eocene caviomorph rodents from Peruvian Amazonia reveal early ecological diversity. *Journal of Vertebrate Paleontology*, **38**, e1555164.

Boivin, M., Marivaux, L. and Antoine, P.-O. 2019. L'apport du registre paléogène d'Amazonie sur la diversification initiale des Caviomorpha (Hystricognathi, Rodentia): implications phylogénétiques, macroévolutives et paléobiogéographiques. *Geodiversitas*, **41**, 143–245.

Brauer, K. and Schober, W. 1970. *Katalog der Säugetiergehirne [Catalogue of mammalian brains]*. Gustav Fischer, 40 pp.

Bugge, J. 1974. Rodentia. 44–78. *In* Bugge, J. (ed.) *The cephalic arterial system in insectivores, primates, rodents and lagomorphs, with special reference to the systematic classification*. Karger, 159 pp.

Bugge, J. 1985. Systematic value of the carotid arterial pattern in rodents. 355–379. *In* Luckett, W. P. and Hartenberger, J.-L. (eds) *Evolutionary relationships among rodents: A multidisciplinary approach*. Springer, 722 pp.

Busker, F. and Dozo, M. T. 2017. First confirmed record of *Incamys bolivianus* (Caviomorpha, Chinchilloidea) in the Deseadan of Patagonia (Argentina). *Ameghiniana*, **54**, 706–712.

Candela, A. M., Rasia, L. L. and Pérez, M. E. 2012. Paleobiology of Santacrucian caviomorph rodents: a morphofunctional approach. 287–305. *In* Bargo, M. S., Kay, R. F. and Vizcaíno, S. F. (eds) *Early Miocene paleobiology in Patagonia: High-latitude paleocommunities of the Santa Cruz Formation*. Cambridge University Press, 370 pp.

Candela, A. M., Muñoz, N. A. and García-Esponda, C. M. 2017. The tarsal–metatarsal complex of caviomorph rodents: anatomy and functional–adaptive analysis. *Journal of Morphology*, **278**, 828–847.

Chambers, J. M. and Hastie, T. J. 1992. *Statistical models in S*. Chapman & Hall, 608 pp.

Charlton, B. D. and Reby, D. 2016. The evolution of acoustic size exaggeration in terrestrial mammals. *Nature Communications*, **7**, 12739.

Chávez Hoffmeister, M. F. 2020. From Gondwana to the Great American Biotic Interchange: the birth of South American fauna. 13–32. *In* Pino, M. and Astorga, G. A. (eds) *Pilauco: A Late Pleistocene archaeo-paleontological site: Osorno, Northwestern Patagonia and Chile*. Springer, 343 pp.

Christensen, G. C. and Evans, H. E. 1979. *Miller's anatomy of the dog*. WB Saunders, 1181 pp.

Dag, O., Dolgun, A. and Konar, N. M. 2018. Onewaytests: an R Package for one-way tests in independent groups designs. *R Journal*, **10**, 175–199.

D'Alessandro, L. M. and Harrison, R. V. 2016. Midbrain frequency representation following moderately intense neonatal sound exposure in a precocious animal model (*Chinchilla laniger*). *Neural Plasticity*, **2016**, 3734646.

Dechaseaux, C. 1958. Encéphales de Simplicidentés fossiles. 819–821. *In* Piveteau, J. (ed.) *Traité de paléontologie: L'origine des mammifères et les aspects fondamentaux de leur évolution*. Masson, Paris, 962 pp.

dos Reis, S. F. and Pessôa, L. M. 2004. Thrichomys apereoides. *Mammalian Species*, **741**, 1–5.

Dozo, M. T. 1997a. Paleoneurología de *Dolicavia minuscula* (Rodentia, Caviidae) y *Paedotherium insigne* (Notoungulata, Hegetotheriidae) del Plioceno de Buenos Aires, Argentina. *Ameghiniana*, **34**, 427–435.

Dozo, M. T. 1997b. Primer estudio paleoneurológico de un roedor caviomorfo (Cephalomyidae) y sus posibles implicancias filogenéticas. *Mastozoología Neotropical*, **4**, 89–96.

Dozo, M. T. and Martínez, G. 2016. First digital cranial endocasts of late Oligocene Notohippidae (Notoungulata): implications for endemic South American ungulates brain evolution. *Journal of Mammalian Evolution*, **23**, 1–16.

Dozo, M. T., Vucetich, M. G. and Candela, A. M. 2004. Skull anatomy and neuromorphology of *Hypsosteiromys*, a Colhuehuapian erethizontid rodent from Argentina. *Journal of Vertebrate Paleontology*, **24**, 228–234.

Dozo, M. T., Martínez, G. and Gelfo, J. N. 2023. Paleoneurology of Litopterna: digital and natural endocranial casts of Macraucheniidae. 809–836. *In* Dozo, M. T., Paulina-Carabajal, A., Macrini, T. E. and Walsh, S. (eds) *Paleoneurology of amniotes: New directions in the study of fossil endocasts*. Springer, 840 pp.

Dunn, R. E., Madden, R. H., Kohn, M. J., Schmitz, M. D., Strömberg, C. A., Carlini, A. A., Ré, G. H. and Crowley, J. 2013. A new chronology for middle Eocene–early Miocene South American land mammal ages. *GSA Bulletin*, **125**, 539–555.

Edinger, T. 1964. Midbrain exposure and overlap in mammals. *American Zoologist*, **4**, 5–19.

Elissamburu, A. and Vizcaíno, S. F. 2004. Limb proportions and adaptations in caviomorph rodents (Rodentia: Caviomorpha). *Journal of Zoology*, **262**, 145–159.

Emmons, L. H. 1981. Morphological, ecological, and behavioral adaptations for arboreal browsing in *Dactylomys dactylinus* (Rodentia, Echimyidae). *Journal of Mammalogy*, **62**, 183–189.

Fernández-Monescillo, M., Antoine, P.-O., Pujos, F., Gomes Rodrigues, H., Mamani Quispe, B. and Orliac, M. 2019. Virtual endocast morphology of Mesotheriidae (Mammalia, Notoungulata, Typotheria): new insights and implications on notoungulate encephalization and brain evolution. *Journal of Mammalian Evolution*, **26**, 85–100.

Fernández Villoldo, J. A., Verzi, D. H., Lopes, R. T., dos Reis, S. F. and Perez, S. I. 2023. Brain size and shape diversification in a highly diverse South American clade of rodents (Echimyidae): a geometric morphometric and comparative phylogenetic approach. *Biological Journal of the Linnean Society*, **140**, 277–295.

Ferreira, J. D., Negri, F. R., Sánchez-Villagra, M. R. and Kerber, L. 2020. Small within the largest: brain size and anatomy of the extinct *Neoepiblema acreensis*, a giant rodent from the Neotropics. *Biology Letters*, **16**, 20190914.

Ferreira, J. D., Dozo, M. T., de Moura Bubadué, J. and Kerber, L. 2022. Morphology and postnatal ontogeny of the cranial endocast and paranasal sinuses of capybara (*Hydrochoerus hydrochaeris*), the largest living rodent. *Journal of Morphology*, **283**, 66–90.

Francescoli, G., Nogueira, S. and Schleich, C. 2016. Mechanisms of social communication in caviomorph rodents. 147–172. *In* Ebensperger, L. A. and Hayes, L. D. (eds) *Sociobiology of caviomorph rodents: An integrative approach*. Wiley Blackwell, 408 pp.

Freeberg, T. M., Dunbar, R. I. M. and Ord, T. J. 2012. Social complexity as a proximate and ultimate factor in communicative complexity. *Philosophical Transactions of the Royal Society B*, **367**, 1785–1801.

Giannini, N. P. and García-López, D. A. 2014. Ecomorphology of mammalian fossil lineages: identifying morphotypes in a case study of endemic South American ungulates. *Journal of Mammalian Evolution*, **21**, 195–212.

Griffiths, B. M., Gilmore, M. P. and Bowler, M. 2020. Predation of a Brazilian porcupine (*Coendou prehensilis*) by an ocelot (*Leopardus pardalis*) at a mineral lick in the Peruvian Amazon. *Food Webs*, **24**, e00148.

Harrison, R. V., Ibrahim, D. and Mount, R. J. 1998. Plasticity of tonotopic maps in auditory midbrain following partial cochlear damage in the developing chinchilla. *Experimental Brain Research*, **123**, 449–460.

Hoffstetter, R. and Lavocat, R. 1970. Découverte dans le Déséadien de Bolivie de genres pentalophodontes appuyant les affinités africaines des Rongeurs Caviomorphes. *Comptes Rendus de l'Académie des Sciences, Paris*, **271**, 172–175.

Hothorn, T., Hornik, K., van de Wiel, M. and Zeileis, A. 2006. A Lego system for conditional inference. *The American Statistician*, **60**, 257–263.

Houle, A. 1999. The origin of platyrrhines: an evaluation of the Antarctic scenario and the floating island model. *American Journal of Physical Anthropology*, **109**, 541–559.

Huchon, D. and Douzery, E. J. 2001. From the Old World to the New World: a molecular chronicle of the phylogeny and biogeography of hystricognath rodents. *Molecular Phylogenetics & Evolution*, **20**, 238–251.

Jackson, J. E., Branch, L. C. and Villarreal, D. 1996. Lagostomus maximus. *Mammalian Species*, **543**, 1–6.

Jerison, H. J. 1961. Quantitative analysis of evolution of the brain in mammals. *Science*, **133**, 1012–1014.

Jerison, H. J. 1973. *Evolution of the brain and intelligence*. Academic Press, 498 pp.

Jerison, H. J. 2012. Digitized fossil brains: neocorticalization. *Biolinguistics*, **6**, 383–392.

Kaas, J. H. 2020. The organization of neocortex in early mammals. 333–348. *In* Kaas, J. H. (ed.) *Evolutionary neuroscience*. Academic Press, 962 pp.

Kay, R. F., MacFadden, B. J., Madden, R. H., Sandeman, H. and Anaya, F. 1998. Revised age of the Salla beds, Bolivia, and its bearing on the age of the Deseadan South American Land Mammal "Age". *Journal of Vertebrate Paleontology*, **18**, 189–199.

Kerber, L., Candela, A. M., Ferreira, J. D., Pretto, F. A., Bubadué, J. and Negri, F. R. 2022. Postcranial morphology of the extinct rodent *Neoepiblema* (Rodentia: Chinchilloidea): insights into the paleobiology of neoepiblemids. *Journal of Mammalian Evolution*, **29**, 207–235.

Klepper, A. and Herbert, H. 1991. Distribution and origin of noradrenergic and serotonergic fibers in the cochlear nucleus and inferior colliculus of the rat. *Brain Research*, **557**, 190–201.

Krubitzer, L., Campi, K. L. and Cooke, D. F. 2011. All rodents are not the same: a modern synthesis of cortical organization. *Brain, Behavior & Evolution*, **78**, 51–93.

Lang, M. M., Bertrand, O. C., San Martin-Flores, G., Law, C. J., Abdul-Sater, J., Spakowski, S. and Silcox, M. T. 2022. Scaling patterns of cerebellar petrosal lobules in Euarchontoglires: impacts of ecology and phylogeny. *The Anatomical Record*, **305**, 3472–3503.

Lavocat, R. 1976. Rongeurs Caviomorphes de l'Oligocène de Bolivie. II. Rongeurs du Bassin Deseadien de Salla-Luribat. *Palaeovertebrata*, **7**, 15–90.

Lima, S. G. C., Sousa-Lima, R. S., Tokumaru, R. S., Nogueira-Filho, S. L. G. and Nogueira, S. S. C. 2018. Vocal complexity and sociality in spotted paca (*Cuniculus paca*). *PLoS One*, **13**, e0190961.

Long, A., Bloch, J. I. and Silcox, M. T. 2015. Quantification of neocortical ratios in stem primates. *American Journal of Physical Anthropology*, **157**, 363–373.

López-Torres, S., Bertrand, O. C., Lang, M. M., Silcox, M. T. and Fostowicz-Frelik, Ł. 2020. Cranial endocast of the stem lagomorph *Megalagus* and brain structure of basal Euarchontoglires. *Proceedings of the Royal Society B*, **287**, 20200665.

Lösel, P. D., van de Kamp, T., Jayme, A., Ershov, A., Faragó, T., Pichler, O., Tan Jerome, N., Aadepu, N., Bremer, S., Chilingaryan, S. A., Heethoff, M., Kopmann, A., Odar, J., Schmelzle, S., Zuber, M., Wittbrodt, J., Baumbach, T. and Heuveline, V. 2020. Introducing Biomedisa as an open-source online platform for biomedical image segmentation. *Nature Communications*, **11**, 5577.

Macrini, T. E., Rougier, G. W. and Rowe, T. 2007. Description of a cranial endocast from the fossil mammal *Vincelestes neuquenianus* (Theriiformes) and its relevance to the evolution of endocranial characters in therians. *The Anatomical Record*, **290**, 875–892.

Madozzo-Jaén, M. C. 2019. Systematic and phylogeny of *Prodolichotis prisca* (Caviidae, Dolichotinae) from the northwest of Argentina (late Miocene–early Pliocene): advances in the knowledge of the evolutionary history of maras. *Comptes Rendus Palevol*, **18**, 33–50.

Mangiafico, S. 2023. rcompanion: functions to support extension education program evaluation. R package v2.4.30. https://CRAN.R-project.org/package=rcompanion/

Marivaux, L., Vélez-Juarbe, J., Merzeraud, G., Pujos, F., Viñola López, L. W., Boivin, M., Santos-Mercado, H., Cruz, E. J., Grajales, A., Padilla, J., Vélez-Rosado, K. I., Philippon, M., Léticée, J.-L., Münch, P. and Antoine, P.-O. 2020. Early Oligocene chinchilloid caviomorphs from Puerto Rico and the initial rodent colonization of the West Indies. *Proceedings of the Royal Society B*, **287**, 20192806.

Marshall, L. G., Hoffstetter, R. and Pascual, R. 1983. Mammals and stratigraphy: geochronology of the continental mammal-bearing Tertiary of South America. *Palaeovertebrata, Mémoire Extraordinaire*, **1983**, 1–93.

Martin, R. D. 1990. *Primate origins and evolution: A phylogenetic reconstruction*. Princeton University Press, 804 pp.

Martínez, G., Dozo, M. T., Vera, B. and Cerdeño, E. 2019. Paleoneurology, auditory region, and associated soft tissue inference in the late Oligocene notoungulates *Mendozahippus fierensis* and *Gualta cuyana* (Toxodontia) from central-western Argentina. *Journal of Vertebrate Paleontology*, **39**, e1725531.

Martínez, G., Macrini, T. E., Dozo, M. T., Vera, B. and Gelfo, J. N. 2023. Endocranial morphology and paleoneurology in notoungulates: braincast, auditory region and adjacent intracranial spaces. 761–807. *In* Dozo, M. T., Paulina-Carabajal, A., Macrini, T. E. and Walsh, S. (eds) *Paleoneurology of amniotes: New directions in the study of fossil endocasts*. Springer, 840 pp.

Maugoust, J. and Orliac, M. J. 2021. Endocranial cast anatomy of the extinct hipposiderid bats *Palaeophyllophora* and *Hipposideros* (*Pseudorhinolophus*) (Mammalia: Chiroptera). *Journal of Mammalian Evolution*, **28**, 679–706.

Meng, J., Hu, Y. and Li, C. 2003. The osteology of *Rhombomylus* (Mammalia, Glires): implications for phylogeny and evolution of Glires. *Bulletin of the American Museum of Natural History*, **275**, 1–247.

Ni, X., Flynn, J. J., Wyss, A. R. and Zhang, C. 2019. Cranial endocast of a stem platyrrhine primate and ancestral brain conditions in anthropoids. *Science Advances*, **5**, eaav7913.

Novacek, M. J. 1986. The skull of leptictid insectivorans and the higher-level classification of eutherian mammals. *Bulletin of the American Museum of Natural History*, **183**, 1–112.

O'Leary, M. A., Bloch, J. I., Flynn, J. J., Gaudin, T. J., Giallombardo, A., Giannini, N. P., Goldberg, S. L., Kraatz, B. P., Luo, Z. X., Meng, J., Ni, X., Novacek, M. J., Perini, F. A., Randall, Z. S., Rougier, G. W., Sargis, E. J., Silcox, M. T., Simmons, N. B., Spaulding, M., Velazco, P. M., Weksler, M., Wible, J. R. and Cirranello, A. L. 2013. The placental mammal ancestor and the post-K-Pg radiation of placentals. *Science*, **339**, 662–667.

Orliac, M. J. and Gilissen, E. 2012. Virtual endocranial cast of earliest Eocene *Diacodexis* (Artiodactyla, Mammalia) and morphological diversity of early artiodactyl brains. *Proceedings of the Royal Society B*, **279**, 3670–3677.

Orliac, M. J., Argot, C. and Gilissen, E. 2012. Digital cranial endocast of *Hyopsodus* (Mammalia, "Condylarthra"): a case of Paleogene terrestrial echolocation? *PLoS One*, **7**, e30000.

Orliac, M. J., Ladevèze, S., Gingerich, P. D., Lebrun, R. and Smith, T. 2014. Endocranial morphology of Palaeocene *Plesiadapis tricuspidens* and evolution of the early primate brain. *Proceedings of the Royal Society B*, **281**, 20132792.

Pacheco de Araújo, A. C. and Campos, R. 2005. A systematic study of the brain base arteries and their blood supply sources in the chinchilla (*Chinchilla lanigera*–Molina 1782). *Brazilian Journal of Morphological Sciences*, **22**, 221–232.

Pascual, R., Ortiz-Jaureguizar, E. and Prado, J. 1996. Land mammals: paradigm for Cenozoic South American geobiotic evolution. *Münchner Geowissenschaftliche Abhandlungen*, **30**, 265–319.

Patterson, B. D. and Wood, A. E. 1982. Rodents from the Deseadan Oligocene of Bolivia and the relationships of the Caviomorpha. *Bulletin of the Museum of Comparative Zoology*, **149**, 371–543.

Patton, J. L., Pardiñas, U. F. J. and D'Elía, G. 2015. *Mammals of South America, Vol. 2: Rodents*. University of Chicago Press, 1362 pp.

Pérez, M. E., Arnal, M., Boivin, M., Vucetich, M. G., Candela, A., Busker, F. and Quispe, B. M. 2019. New caviomorph rodents from the late Oligocene of Salla, Bolivia: taxonomic, chronological, and biogeographic implications for the Deseadan faunas of South America. *Journal of Systematic Palaeontology*, **17**, 821–847.

Perini, F. A., Macrini, T. E., Flynn, J. J., Bamba, K., Ni, X., Croft, D. A. and Wyss, A. R. 2022. Comparative endocranial anatomy, encephalization, and phylogeny of Notoungulata (Placentalia, Mammalia). *Journal of Mammalian Evolution*, **29**, 369–394.

Pessôa, L. M., Tavares, W. C., Oliveira, J., Patton, J. L., Pardiñas, U. and D'elía, G. 2015. Genus *Trinomys* Thomas, 1921. *Mammals of South America*, **2**, 999–1019.

Petersen, C. L. and Hurley, L. M. 2017. Putting it in context: linking auditory processing with social behavior circuits in the vertebrate brain. *Integrative & Comparative Biology*, **57**, 865–877.

Petry, H. M. and Bickford, M. E. 2019. The second visual system of the tree shrew. *Journal of Comparative Neurology*, **527**, 679–693.

Pilleri, G., Gihr, M. and Kraus, C. 1984. Cephalization in rodents with particular reference to the Canadian beaver (*Castor canadensis*). *In* Pilleri, G. (ed.) *Investigations on beavers. Vol. 2*. Brain Anatomy Institute, Berne, 102 pp.

Piñero, P., Verzi, D. H., Olivares, A. I., Montalvo, C. I., Tomassini, R. L. and Fernández Villoldo, A. 2021. Evolutionary pattern of *Metacaremys* gen. nov. (Rodentia, Octodontidae) and its biochronological implications for the late Miocene and early Pliocene of southern South America. *Papers in Palaeontology*, **7**, 1895–1917.

Pinheiro, J., Bates, D., Debroy, S. and Sarkar, D. 2023. nlme: linear and nonlinear mixed effects models. R package v3.1-162. https://CRAN.R-project.org/package=nlme

Portfors, C. V. and Sinex, D. G. 2005. Coding of communication sounds in the inferior colliculus. 411–425. *In* Winer, J. A. and Schreiner, C. E. (eds) *The inferior colliculus*. Springer, 705 pp.

R Core Team. 2019. R: a language and environment for statistical computing. R Foundation for Statistical Computing. https://www.R-project.org/

R Studio Team. 2022. RStudio: integrated development environment for R. http://www.rstudio.com

Rambold, H., Churchland, A., Selig, Y., Jasmin, L. and Lisberger, S. G. 2002. Partial ablations of the flocculus and ventral paraflocculus in monkeys cause linked deficits in smooth pursuit eye movements and adaptive modification of the VOR. *Journal of Neurophysiology*, **87**, 912–924.

Rasia, L. L. and Candela, A. M. 2019. Upper molar morphology, homologies and evolutionary patterns of chinchilloid rodents (Mammalia, Caviomorpha). *Journal of Anatomy*, **234**, 50–65.

Rasia, L. L., Candela, A. M. and Cañón, C. 2021. Comprehensive total evidence phylogeny of chinchillids (Rodentia, Caviomorpha): cheek teeth anatomy and evolution. *Journal of Anatomy*, **239**, 405–423.

Rinderknecht, A. and Blanco, R. E. 2008. The largest fossil rodent. *Proceedings of the Royal Society B*, **275**, 923–928.

Rowe, T. B., Macrini, T. E. and Luo, Z. X. 2011. Fossil evidence on origin of the mammalian brain. *Science*, **332**, 955–957.

Shultz, S. and Dunbar, R. I. M. 2006. Both social and ecological factors predict ungulate brain size. *Proceedings of the Royal Society B*, **273**, 207–215.

Sibly, R. M. and Brown, J. H. 2009. Mammal reproductive strategies driven by offspring mortality–size relationships. *The American Naturalist*, **173**, E185–E199.

Silcox, M. T., Dalmyn, C. K. and Bloch, J. I. 2009. Virtual endocast of *Ignacius graybullianus* (Paromomyidae, Primates) and brain evolution in early primates. *Proceedings of the National Academy of Sciences*, **106**, 10987–10992.

Silcox, M. T., Benham, A. E. and Bloch, J. I. 2010. Endocasts of *Microsyops* (Microsyopidae, Primates) and the evolution of the brain in primitive primates. *Journal of Human Evolution*, **58**, 505–521.

Sobrero, R., Inostroza-Michael, O., Hernández, C. E. and Ebensperger, L. A. 2014. Phylogeny modulates the effects of ecological conditions on group living across hystricognath rodents. *Animal Behaviour*, **94**, 27–34.

Sol, D., Bacher, S., Reader, S. M. and Lefebvre, L. 2008. Brain size predicts the success of mammal species introduced into novel environments. *The American Naturalist*, **172**, S63–S71.

Spoor, F., Garland, T., Krovitz, G., Ryan, T. M., Silcox, M. T. and Walker, A. 2007. The primate semicircular canal system and locomotion. *Proceedings of the National Academy of Sciences*, **104**, 10808–10812.

Spotorno, A. E., Zuleta, C. A., Valladares, J. P., Deane, A. L. and Jiménez, J. E. 2004. Chinchilla laniger. *Mammalian Species*, **758**, 1–9.

Stehli, F. G. and Webb, S. D. 1985. *The Great American Biotic Interchange*. Springer, Topics in Geobiology, 532 pp.

Tambusso, P. S. and Fariña, R. A. 2015a. Digital cranial endocast of *Pseudoplohophorus absolutus* (Xenarthra, Cingulata) and its systematic and evolutionary implications. *Journal of Vertebrate Paleontology*, **35**, e967853.

Tambusso, P. S. and Fariña, R. A. 2015b. Digital endocranial cast of *Pampatherium humboldtii* (Xenarthra, Cingulata) from the Late Pleistocene of Uruguay. *Swiss Journal of Palaeontology*, **134**, 109–116.

Upham, N. and Patterson, B. 2015. Evolution of caviomorph rodents: a complete phylogeny and timetree for living genera. 63–120. *In* Vassallo, A. and Antenucci, D. (eds) *Biology of caviomorph rodents: Diversity and evolution*. Sociedad Argentina para el estudio de los Mamíferos, Buenos Aires, 329 pp.

Vandenberghe, N., Hilgen, F. J., Speijer, R. P., Ogg, J. G., Gradstein, F. M., Hammer, O., Hollis, C. J. and Hooker, J. J. 2012. The Paleogene period. 855–921. *In* Gradstein, F. M., Ogg, J. G., Schmitz, M. D. and Ogg, G. M. (eds) *The geologic time scale*. Elsevier, 1176 pp.

Verzi, D. H., Álvarez, A., Olivares, A. I., Morgan, C. C. and Vassallo, A. I. 2010. Ontogenetic trajectories of key morphofunctional cranial traits in South American subterranean ctenomyid rodents. *Journal of Mammalogy*, **91**, 1508–1516.

Visualization Sciences Group. 1995–2019. Avizo Lite 2019.4.

Vucetich, M., Arnal, M., Deschamps, C., Pérez, M. and Vieytes, E. 2015a. A brief history of caviomorph rodents as told by the fossil record. 11–62. *In* Vassallo, A. and Antonucci, D. (eds) *Biology of caviomorph rodents: Diversity and evolution*. Sociedad Argentina para el estudio de los Mamíferos, Buenos Aires, 329 pp.

Vucetich, M. G., Deschamps, C. M. and Pérez, M. E. 2015b. The first capybaras (Rodentia, Caviidae, Hydrochoerinae) involved in the Great American Biotic Interchange. *Ameghiniana*, **52**, 324–333.

Vucetich, M. G., Dozo, M. T., Arnal, M. and Pérez, M. E. 2015c. New rodents (Mammalia) from the late Oligocene of Cabeza Blanca (Chubut) and the first rodent radiation in Patagonia. *Historical Biology*, **27**, 236–257.

Welch, B. L. 1951. On the comparison of several mean values: an alternative approach. *Biometrika*, **38**, 330–336.

White, C. L., Bloch, J. I., Morse, P. E. and Silcox, M. T. 2023. Virtual endocast of late Paleocene *Niptomomys* (Microsyopidae, Euarchonta) and early primate brain evolution. *Journal of Human Evolution*, **175**, 103303.

Wible, J. R. 1990. Petrosals of Late Cretaceous marsupials from North America, and a cladistic analysis of the petrosal in therian mammals. *Journal of Vertebrate Paleontology*, **10**, 183–205.

Wible, J. R. and Shelley, S. L. 2020. Anatomy of the petrosal and middle ear of the brown rat, *Rattus norvegicus* (Berkenhout, 1769) (Rodentia, Muridae). *Annals of Carnegie Museum*, **86**, 1–35.

Wickham, H. 2016. *ggplot2: Elegant graphics for data analysis*. Springer, 260 pp.

Wood, A. E. 1974. Early Tertiary vertebrate faunas, Vieja Group, Trans-Pecos Texas: Rodentia. *The Bulletin of the Texas Memorial Museum*, **21**, 112 pp.